Universidade de Aveiro Departamento de Química

2014

Adriana Filipa da Silva Fontes

Defeitos mitocondriais em mutantes proteasomais e do COP9

Mitochondrial defects in proteasome and COP9 mutants

Universidade de Aveiro **Departamento de Química**

2014

Adriana Filipa da Silva Fontes

Defeitos mitocondriais em mutantes proteasomais e do COP9

Mitochondrial defects in proteasome and COP9 mutants

Dissertação apresentada à Universidade de Aveiro para cumprimento dos requisitos necessários à obtenção do grau de Mestre em Biotecnologia no ramo de Biotecnologia Molecular, realizada sob a orientação científica da Doutora Teresa Rinaldi, Professora do Departamento Biologia e Biotecnologia Charles Darwin da Universidade de "La Sapienza" e da Doutora Etelvina Figueira, Professora do Departamento de Biologia da Universidade de Aveiro

Dedico este trabalho à minha família, em especial aos meus pais por todo o apoio que me deram nesta jornada e porque sem eles nada disto seria possível, aos meus amigos, à Soraia pela força e ao Aléxis por todos os dias ter estado do meu lado.

o júri

presidente Prof. Doutor Henrique Manuel Apolónia Coutinho da Fonseca

Professor Auxiliar do Departamento de Biologia da Universidade de Aveiro

Prof. Doutora Etelvina Maria de Almeida Paula Figueira

Professora Auxiliar do Departamento de Biologia da Universidade de Aveiro

Doutora Maria Fátima Camões

Investigadora no Centro de Biologia Celular da Universidade de Aveiro

agradecimentos Quero agradecer à Professora Teresa Rinaldi pela confiança demonstrada em aceitar me no seu grupo de investigação, pelo conhecimento científico e apoio disponibilizado durante estes meses de trabalho.

Aos meus colegas de laboratório: Rosa Santomartino, Angela Cirigliano e Alessandro Stirpe, que se tornaram amigos e me ajudaram, incansavelmente, em tudo o que precisei.

palavras-chave Proteasoma, COP9 signalosome, SCF E3 ligase, CSN5, mitocôndria, *Saccharomyces cerevisiae*

resumo O objectivo deste trabalho centrou-se no estudo das alterações fenotípicas e ao nível da morfologia mitocondrial em células de levedura *Saccharomyces cerevisiae* com mutações específicas em genes envolvidos na via de degradação proteica ubiquitina-proteasoma. O *turnover* proteíco é muito importante pois garante a viabilidade dos vários organelos celulares, de entre os quais, a mitochondria, cuja função principal é a produção de energia na forma de ATP. A subunidade Csn5 do COP9 signalosome, complexo com elevada similaridade com a *lid* proteasomal e com o factor 3 de iniciação translacional em eucariotas (eIF3), é responsável pela actividade da E3 ligase Cdc53/Cul1 através da remoção da proteina similar à ubiquitina, Rub1. A delação do gene que codifica para a subunidade Csn5 é letal em eucariotas superiores mas não em levedura o que nos permite estudar os seus efeitos juntamente com outros mutantes: rpn11-m1, Δrub1, rpn11-m1/Δcsn5 rpn11-m1/ Δrub1. Mutantes e *wild-type* (W303-1A) foram caracterizados a nível de crescimento em diferentes fontes de carbono e a diferentes temperaturas, assim como à resposta a factores causadores de dano ao nível do DNA e síntese proteica (sulfonato de metil metano e canavanina) juntamente com uma análise do potencial de membrana mitochondrial, autofagia/mitofagia através de microscopia de fluorescencia (GFP-Atg8 e GFP-Atg32) e Western Blot. Os resultados obtidos indicam que existe uma relação entre a acção de deubiquitinação da proteina Rpn11, da subunidade 19S do proteasome, e a activação dos ciclos de rubilação/derubilação pela subunidade Csn5 do complex CSN (COP9 signalosome), sendo que o mutante rpn11-m1/Δrub1 apresenta um fenótipo semi-letal com instabilidade ao nível do DNA e alterações mitocôndriais que levam a um mitofagia em fase exponencial em meio rico em glucose. Por sua vez, o mutante rpn11-m1/Δcsn5 também revela mitofagia prematura em conjunto com alterações fenotípicas, como o aumento da dimensão celular (grande vacúolo), que ja é também evidente no mutante Δcsn5. Foi ainda estabelecida uma possível relação entre o complex CSN e a capacidade de resistência aos danos causados no DNA pelo agente metilante MMS.

keywords Proteasoma, COP9 signalosome, SCF E3 ligase, CSN5, mitochondrion, *Saccharomyces cerevisiae*

abstract The aim of this work is the study of phenotypic changes and mitochondrial morphology in *Saccharomyces cerevisiae* cells with specific mutations in genes involved in the ubiquitin-proteasome pathway. The protein turnover is important because it ensures organelles viability such as mitochondria, indispensable for cell survival. The COP9 complex is paralogous to the proteasome lid and eukaryotic translational initiator factor 3 (eIF3) complexes. The CSN5 subunit of the COP9 signalosome is responsible for the E3 ligase Cdc53/Cul1 activity through the removal of the ubiquitin-like protein, Rub1. Deletion of the Csn5 gene is lethal in high eukaryotes but not in yeast, this observation allow us to study the effects of this mutation in this organism (strain Δcsn5) together with other mutants or double mutants: rpn11-m1, Δrub1, rpn11-m1/Δcsn5 rpn11-m1/ Δrub1. Mutants and wild-type (W303-1A) were characterised regarding growth in different carbon sources and temperature as well as response to stress or DNA damage causing agents (methyl methanesulfonate and canavanin). The morphological results allowed us to investigate authophagy, and in particular mitophagy, through fluorescence microscopy (GFP-Atg8 and GFP-Atg32) and Western Blot analysis. We found a relation between deubiquitination undertaken by Rpn11 protein, from the 19S proteasome subunit, and the activation of rubylation/derubylation cycles by the CSN5 subunit of the CSN complex (COP9 signalosome). In fact, the rpn11-m1/ Δrub1 shows a semi-lethal phenotype and mitophagy in exponential phase in glucose rich medium. Also the Δcsn5 strain shows early mitophagy together with phenotypic changes, such as big vacuoles. In addition, it has been established a possible relationship between the CSN complex and the resilience to damage in the DNA caused by the methylating agent, methyl methanesulfonate (MMS).

Table of contents

Table of figures

Table of tables

Abbreviations list

COP9 – Constitutive photomorphogenesis 9

CSN – COP9 signalosome complex

UPS – Ubiquitin-proteasome system

eIF3 – Eukaryotic translational initiation factor 3

Ub - Ubiquitin

UBL – Ubiquitin-like proteins

DUBs – Deubiquitinating enzymes

RING – Really interesting new gene

CRLs – Cullin-Ring ligases

SCF – Skp-cullin-F box containing complex

E1 – Ubiquitin-activating enzyme

E2 – Ubiquitin-Conjugating enzyme

E3 – Ubiquitin protein ligases

NEDD8 – Neural precursor cell expressed, developmentally down regulated 8

Rub1 – Related to ubiquitin

DNA – deoxyribonucleic acid

mtDNA – mitochondrial DNA

ATP – adenosine tri-phosphate

ROS – reactive oxygen species

SD – Synthetic media

WT – Wild type

YP – Yeast peptone extract

GFP – Green fluorescence protein

1. Introduction

The COP9 signalosome (constitutive photomorphogenesis 9 signalosome), also known as CSN complex, is a highly conserved protein complex from yeast to humans. It has structural and functional similarities with the 26S proteasome lid and the eukaryotic translation initiation factor 3 (eIF3) and functions in the ubiquitin-proteasome pathway regulating the activity of a specific type of ubiquitin E3 ligases, the cullin-RING ligase (CRL) familiy. This regulation is based on the removal of the ubiquitin-like protein Nedd8 (known as Rub1 in budding yeast), by a deneddylase activity of the CSN subunit 5 (Csn5). This enzyme contains an active metal binding MPN+/JAMM metalloprotease motif. In the proteasome lid, the deubiquitinating enzyme, Rpn11 is the Csn5 paralog that is essential for maintaining a correct cell cycle and mitochondrial morphology in the model organism *Saccharomyces cerevisiae*.

Apart from plants, insects and mammals, *S.* cerevisiae can survive without the CSN complex given us the possibility to study subunit mutations in a living cell. In the other hand, is also very useful in the study of mitochondrial defects due to its capacity of performing fermentation.

The mitochondrion, as the organelle that provides cell with energy (ATP) being critical for cell survival and main actor in several human diseases, is also very sensitive to mutations and lesions due to ROS production and therefore, misfolded/non-functional proteins degradation is essential to maintain a correct function.

Relying on preliminary studies, the aim of this work is, in a first moment, to investigate cell phenotypes in a Wild-type (W303) strain and in the following single and double mutants: Δcsn5, rpn11-m1, Δrub1, rpn11-m1/Δcsn5 and rpn11-m1/Δrub1 in order to study the influence of this mutants in yeast cell growth, vitality, vacuolar phenotype, cell cycle progression and mitochondria morphology. After this, the study of a specific type of autophagy, mitophagy will follow to understand if, in the case of double mutants rpn11-m1/Δcsn5 and rpn11-m1/Δrub1 we have a cumulative defect on the rubylation/derubylation cycles and therefore a decrease in protein degradation by the proteasome due to the lack of cullin-RING activation that can lead to mitochondrion defects. This approach is important to know if the Rpn11 subunit of the proteasome lid plays a role in the deneddylation/derubylation along with Csn5, which could allow the establishment of a relationship between the 26S proteasome and the CSN complex in the ubiquitin-proteasome pathway.

2. Bibliographic Review

2.1 Ubiquitin-Proteasome system

The degradation of the protein waste is a central mechanism for the maintenance of cell viability. Due to transcription and translation errors, genomic mutations or diverse genetic conditions, non functional proteins can accumulate in the cell forming aggregates that can be associated with toxicity therefore altering the natural cell environment [1]. Being the major workers, proteins are required for several processes such as, cell cycle progression, signaling, cell movement, transport, protection, catalysis regulation, homeostasis, among others. However, a high collaboration is needed among molecular chaperones and targeted protein degradation systems, the protein quality control (PQC) acts in order to keep a balance in the cell metabolism [1,2].

Elimination of misfolded proteins is carried by the Ubiquitin Proteasome System (UPS) and by the Autophagic Vacuolar (lysosomal) System (AVS). While autophagy is a mechanism of long-living cytosolic proteins and organelles degradation, the proteasome centers its action in specific short-living proteins [1,2,3].

2.1.1 The role of Ubiquitin in protein degradation

Regarding the UPS, a 76 amino acid protein named ubiquitin (Ub) tags proteins for degradation by the proteasome, through the formation of polyUb chains that are linked by an isopeptide bond between the C-terminus of ubiquitin and the ε-amino group of a lysine side chain in the substrate [1,4]. Lysine residues in the protein are targets for ubiquitylation and it was once thought that a Lys48-based chain of ubiquitin was strictly necessary for the protein-protein interaction that leads to proteasome recognition. However, new evidences show that the mechanism is more complex and even a monoubiquitylated protein can be recognized and other residues than Lys can link ubiquitinated enlightening a high adaptability of the UPS [1,4]. But, in the case of monoubiquitylation, this post-translational modification can regulate target activity instead of enforcing its destruction [5]. Interestingly, the UPS system also evolved to be able to recognize, not just Ub, but also Ubiquitin-like proteins (Ubls), whose functions go beyond protein cell targeting degradation. Examples of Ubls are the small ubiquitin modifier (SUMO) and the neural precursor cell expressed, developmentally downregulated 8 (NEDD8)[5,6,7]. However, this adaptability of the UPS

can turn against it, delivering a lack of accuracy where the proteasome is induced to degrade functional proteins. This fact together with aberrations in the Ub system and the accumulation of misfolded proteins are linked to some pathologies ranging from neurodegenerative diseases like Parkinson, Alzheimer and Huntington to immune and inflammatory disorders such as type 2 diabetes and also cancer, where alterations in the machinery involved in linking or removing ubiquitin to specific substrates can occur in tumor-suppressor proteins [1,4,5,8]. Hershko A., *et al* (1992) highlighted the ubiquitin-dependent degradation mechanism showing that ubiquitin does not work alone but that are a set of ubiquitin conjugating enzymes allowing the entire process from the ubiquitin targeting until the protein degradation. These enzymes are the ubiquitin-activating enzyme (E1), the ubiquitin-conjugating enzymes (E2) and the ubiquitin-protein ligases (E3), which together perform the ubiquitination [1,9,10].

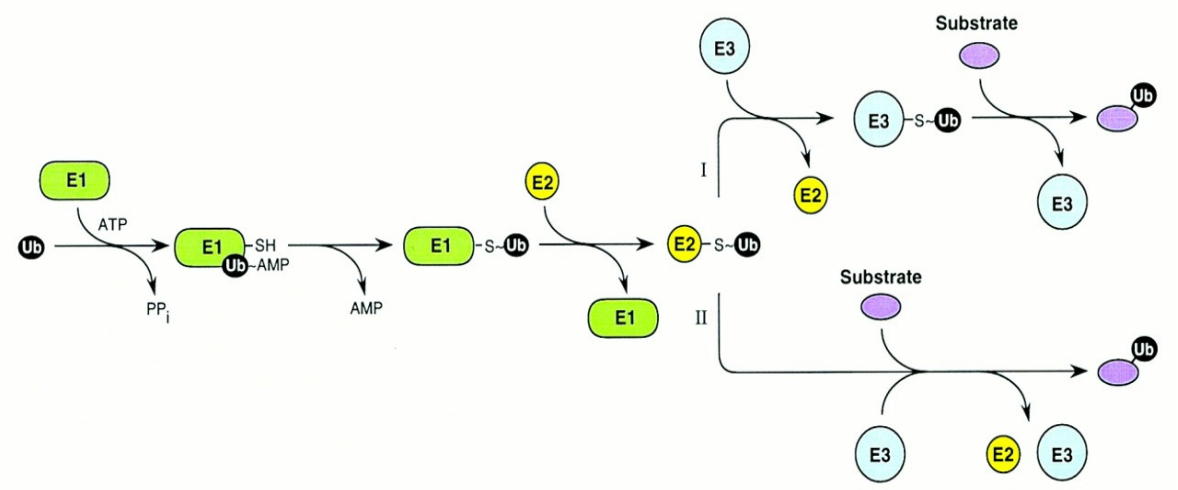

Figure 1. Schematic representation of the ubiquitin conjugation pathway. Formation of the thioester bond mediated by the E1 with ATP expend followed by the conjugation with a reactive cysteine of a second enzyme, E2. The next step requires the aid of a third enzyme, an E3. Two pathways are considered for this last step: (I) Ubiquitin is transferred to the thiol group of the E3 enzyme and only then is conjugated with the substrate; (II) For other E3, the enzyme seems to work more as an adaptor, juxtaposing the E2-ubiquitin thiolester and substrate to allow transfer of ubiquitin directly from E2 [11].

2.1.2 The 26S proteasome

The ubiquitin/proteasome pathway is one of the most conserved regulatory pathways among eukaryotes and the proteasome structure exhibit >40% identity between yeast and humans. Some key components can share 70-80% of similarity with human homologs rescuing knockouts of yeast proteasomal genes [9]. Also in archaea and bacteria proteasomes are present but with less structural complexity [10].

Two major subcomplexes constitute the 26S proteasome, a 20S barrel-shaped structure made up of four heptagonal rings consisting of two inner catalytic rings (β 1-7) and two outer regulatory rings (α 1-7) and a 19S regulatory particle that is composed by a lid and a base [4, 9-12]. The base is composed of six ATPases-Rpt1-6, Rpn1, Rpn2 and two ubiquitin receptors, Rpn10/S5a and Rpn13 being the Rpn10 subunit responsible for the connection with the lid. In its turn, the lid contains the remaining Rpn subunits (Rpn5, Rpn6, Rpn7, Rpn8, Rpn9, Rpn11 and Rpn12), of which only Rpn11 is known to have a deubiquitinating activity [4, 10]. The functions of the 19S regulatory complex are mainly related with the recognition and translocation of misfolded proteins to the 20S complex in which they are degradated by the proteolytic β subunits [10]. This massive holoenzyme with 1.5 MDa is the center of the proteolysis controlling a myriad of cellular processes but yet it does not work alone [9,12].

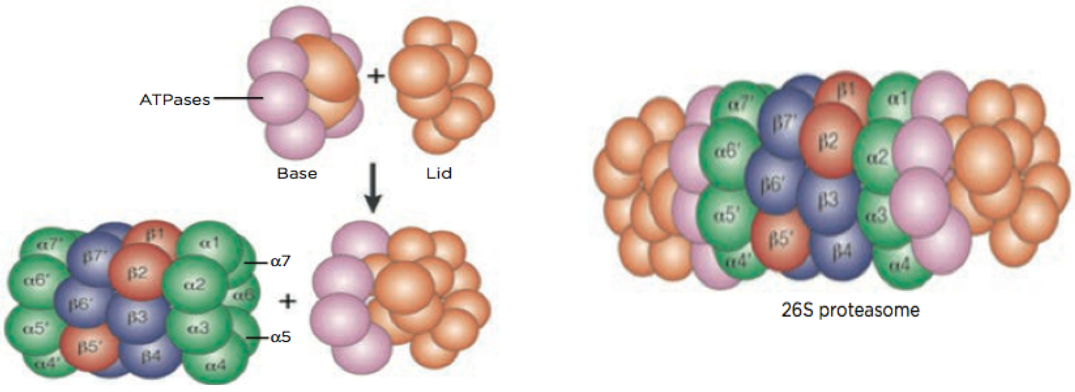

Figure 2. Representation of the 26S proteasome. The base and the lid form the 19S regulatory complex that is added to the 20S core composed by the inner β catalityc rings and the outer α regulatory rings to form the 26S proteasome complex [13].

2.1.3 Steps for ubiquitination

A cascade of events occur during the ubiquitination, and as first described in the Figure 1, it begins with the action of an E1 enzyme, with ATP expend, forming an energy-rich thioester bond with the C-terminal glycine residue of ubiquitin and the active site cysteine of the enzyme. After, the ubiquitin residue is transferred to the active site cysteine of an E2 enzyme and finally, with the help of an E3 enzyme the ubiquitin is linked to the lysine side chain of the protein to creating an isopeptide bond [1,9,11].

A big diversity can be found regarding E1, E2 and E3 enzymes, which is consistent with what it was already said about the high adaptability of the ubiquitin-proteasome system. The ubiquitination process is just the first step for the protein degradation. It is then necessary to deliver the ubiquitinated protein to the proteasome and sometimes intermediates are needed such as extra-proteasomal Ub receptors. They are composed by one Ub-like domain (UBL), that binds the 26S proteasome, and one Ub associated domain (UBA) that binds polyubiquitinated proteins [2,6]. As well as a protein can be ubiquitinated it can also be deubiquitinated by specific enzymes called deubiquitinating enzymes (DUBs) which main function is the removal of ubiquitin residues linked to the substrate therefore promoting Ub recycling [2].

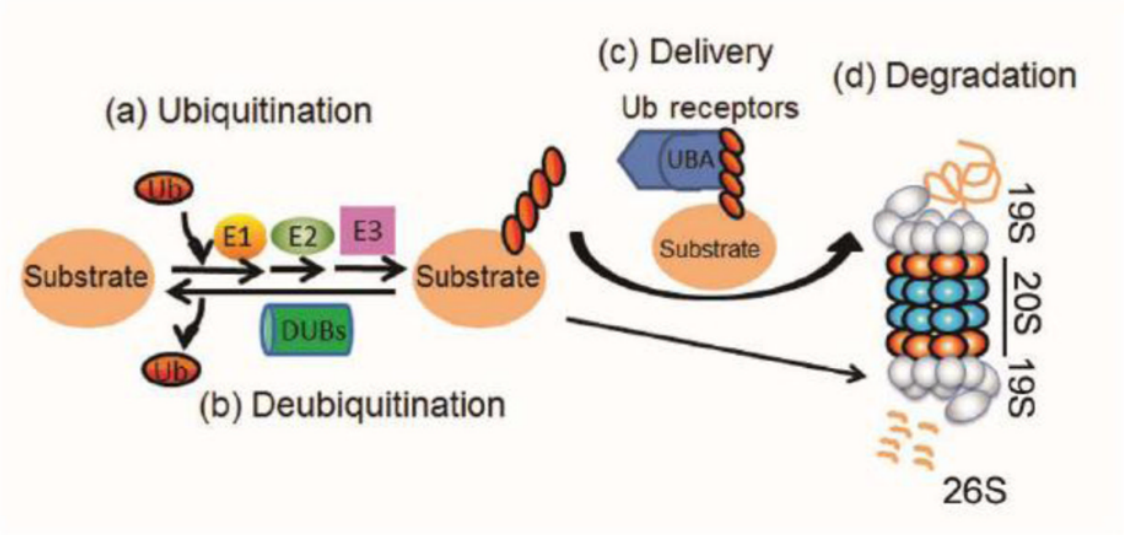

Figure 3. Schematic representation of the ubiquitin-proteasome pahtway. (a) Ubiquitination process mediated by the enzymatic machinery,E1, E2 and E3 enzymes. (b) Removal of the ubiquitin residues trough the action of deubiquitinating enzymes (DUBs). (c) Delivery of the protein by Ub receptors for proteasome degradation (d). The protein is recognize by the ubiquitin receptorslocated in the 19S base, then is translocate by the α rings subunits (orange) to the center of the 20S subunit to be degraded in the catalytic core, the β rings (blue). At the end, polypeptides are release from the 26S proteasome [2].

The proteasomal integral DUB, Rpn11, located in the 19S lid, detains a highly conserved MPN+ (Mpr1, Pad1, N-terminal)/JAMM (JAB1/MPN/Mov34) domain-associated metalloisopeptidase [12,14]. It removes polyubiquitin chains from substrates, a prerequisite for their future processing [15]. But this proteasome subunit has other functions besides deubiquitination. Rinaldi T., *et al* (1998) developed some studies in *Saccharomyces cerevisae* regarding Rpn11 that were focused in a specific missense mutation, mpr1-1, after renamed rpn11-m1. This mutation causes a frame shift, producing a premature C-terminal ending, resulting in a truncated protein missing the last 31 amino acids [14,16]. In this study, they showed, for the first time, that a proteasomal mutation could be associated with changes in mitochondrial phenotype [18]. Pleiotropic effects such as elongated yeast cells containing multiple punctate mitochondrial structures were observed at 36ºC, together with an undivided nucleus in the bud. These results demonstrate the role of the protein Rpn11 in the cell cycle control due to G_2-M phase arrest in the mutant strains after shift to 36ºC, delay that is caused by the failure in the release of the Cdc14 protein phosphatase from the nucleus in the mother cell before anaphase during FEAR (CDC fourteen early anaphase release) pathway [1,17,18]. In several cases, these mutations were accompanied by the accumulation of ubiquitinated proteins, which is due to the deubiquitinase activity of Rpn11 [18].

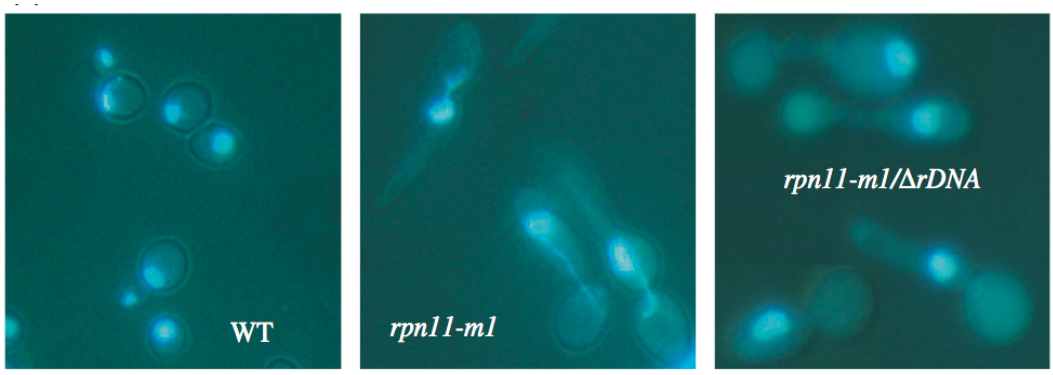

Figure 4. Observation of nuclear DNA through DAPI staining in the rpn11-m1 proteasomal mutant, comparing with wilp-type and rpn11-m1/ΔrDNA cells. We see a clearly change in cell morphology and a pre-anaphase arrest with unsegregated chromosomes that migrate into the elongated bud [17].

Previously, Rinaldi T., *et al* (2008) elaborated a careful study about the Rpn11-m1 mutant and its influence in mitochondria biogenesis and morphology [16]. They observed

that a specific α-motif downstream the 31 amino acid sequence missing in rpn11-m1, is necessary for the maintenance of a correct cell cycle, while only four amino acids are necessary for maintaining the correct mitochondrial morphology.

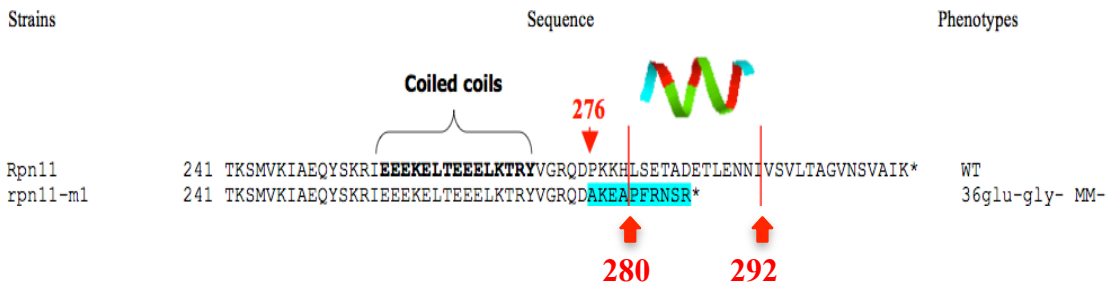

Figure 5. Comparison between Rpn11 and rpn11-m1 C-terminal which specific sequences can be found in blue. Site-directed mutagenesis to introduce a deletion at position 256-270 (coiled coils) seems to induce pleiotropic phenotypes while the missing-sequence in the rpn11-m1 alone may account for mitochondrial and cell cycle phenotypes. From the position 280 to the 292 is represented the α-motif[16].

In another interesting study, Hofmann L., *et al* (2009), attribute another function to this proteasomal protein, a role in the mitochondrial fission [19]. They established that Rpn11 regulates the Fis1-dependent machinery (Fis/Mdv1/Caf4/Dnm1) that is common to both mitochondria and peroxisomes, based on mutational studies using the rpn11-m1 mutation together with strains deleted of genes involved in the fission events (Δfis1, Δdnm1 and Δvps1) [19].

A study in mammalian cells also show that Rpn11-overexpression affects cell proliferation and the response of cytotoxic drugs used in cancer treatments which promote tumor cell escape [20].

2.1.4 The Cullin-Ring Ligases

As we have seen, the ubiquitin-proteasome system is responsible for the specific and timely removal of regulatory proteins involved in essential cellular functions [7, 15]. Substrate interactions are a critical point in the process and because of that a high level of ubiquitin-ligases (E3) diversity provide individuality to the ubiquitin cascade reactions

[21]. The E3 enzymes fall into three classes that can bear a HECT (homologous to E6-AP carboxy terminus), a RING (really interesting new gene) or a U-box domain that is structurally and functionally similar to the RING [6,7,21]. The RING-finger contains two zinc atoms held by seven cysteines and one histidine, or six cysteine and two histidine residues and in total it comprises 40-60 residues being the largest E3 ligase domain [5,21]. It was first linked to the ubiquitin-proteasome system through its discovery in subunits of two cell cycle-regulatory E3-ligases: APC/C (Anaphase promoting complex/Cyclosome) and the SCF (Skp1-Cullin-F-box)[5,6]. Within RING finger E3s there are 2 subclasses: the simple RING finger that contains the E2-binding RING domain and the substrate-binding domain together in the same polypeptide and the cullin-RING ligases (CRLs)[22].

The Cullin-RING ubiquitin ligases are the largest known class regulating diverse cellular processes such as cell cycle, transcription and development [23]. CRLs include a cullin, a RING H2 finger, a substrate-recognition subunit (SRS) and an adaptor to link the SRS to the protein complex [21,23]. They are activated by the covalent attachment of the ubiquitin-like protein NEDD8 to the cullin, a process called neddylation. In turn, the inhibition is performed by a cullin-associated and neddylation-dissociated 1 (CAND1) that binds the cullin in the absence of NEDD8 preventing the neddylation [24]. Besides this regulation mechanism, the formation of CRLs dimers also shows to be a potential source of regulation [23].

The SCF ubiquitin ligase complex was first identified together in budding yeast and *C. elegans* through genetic studies in cell division [6,25]. After structural analysis the pieces of the complex were revealed: a cullin scaffold subunit, the smaller adaptor Skp1, a F-box protein and a RING H2 finger protein Rbx1/Roc1/Hrt1 [23]. There are five major categories of cullins in metazoan (CUL1-CUL5) being the CUL1 the most studied Cullin-RING ubiquitin ligase (CRL) with the budding yeast ortholog, Cdc53 [5,6,7,23].

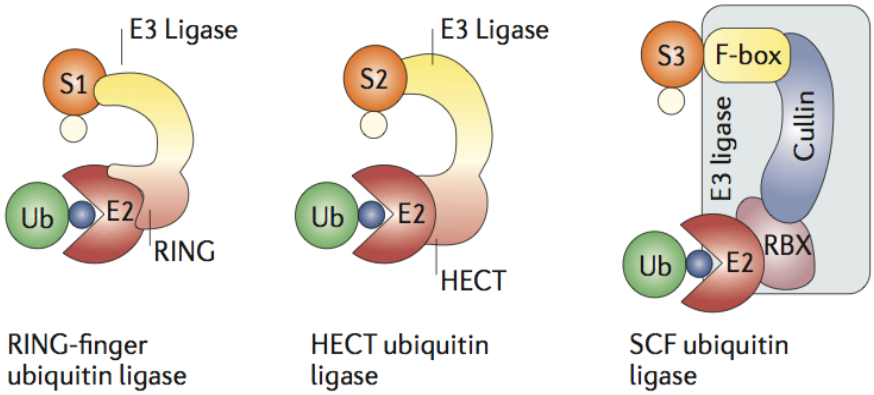

Figure 6. Representation of the ubiquitin ligase classes: RING-finger, HECT and SCF ubiquitin ligase. Regarding the SCF E3 complex it consists in a scaffold-like cullin molecule, a F-box that is the linking-substrate module and a RING-finger containing subunit (RBX1) that in turn binds the ubiquitin-conjugating enzyme (E2) that carries the ubiquitin residue (Ub)[5].

The F-box protein plays an important role in protein destruction due to the direct interaction with the substrates. The majority interacts with specific targets depending on post-translational modifications that it might have, for example phosphorylation, is the most common [5,26]. A SCF ubiquitin ligase can be characterized based on the F-box being the most prominent the SCF^{SKP2}, $SCF\beta^{-TRCP}$ and SCF^{FBW7}. For example, the F-box SKP2 is specialized in the degradation of several negative cell-cycle regulators, such as the cyclin-dependent kinase inhibitor p27 or the p130 and therefore when overexpressed can act as an oncogene by targeting this proteins for degradation by the UPS [5,9]: dysregulation of p27 expression occurs in various cancers [22].

As we saw before, NEDD8 has a role in the CRLs activation allowing the translocation of the ubiquitin residues to the substrate. The NEDD8 conjugation is catalyzed by a specific E1-like heterodimer (ULA1-UBA) named NEDD8-activating enzyme (NAE) that delivers the activated protein to an E2 enzyme called UB12, via a transthiolation reaction [6,22,24]. The latter stage of neddylation is not clear yet but it has been suggested that RBX1 has a E3-type ligase activity for cullin-1 neddylation and regulates poly-NEDD8 chain formation [27]. In fact, all the process underlying NEDD8 influence in the UPS pathway is being discussed. It is also thought that NEDD8 does not interact directly with

the E2-conjugating enzyme but instead it binds to the cullin C-terminal catalytic domain inducing a conformational change in the complex that diminishes the distance between the activated E2 enzyme and the substrate, stimulating ubiquitination [6,28]. In practical example, neddylation enhances the activity of the $CRL1^{SKP2}$ towards p27, an important cell cycle regulator [29] and is also essential for IκBα ubiquitination by $CRL1\beta^{-TRCP}$, a process that allows the translocation of the NF-κB factor into the nucleus, where it activates the expression of important genes for cytokine and cell survival responses, for example, inflammatory response [5,6,23,27].

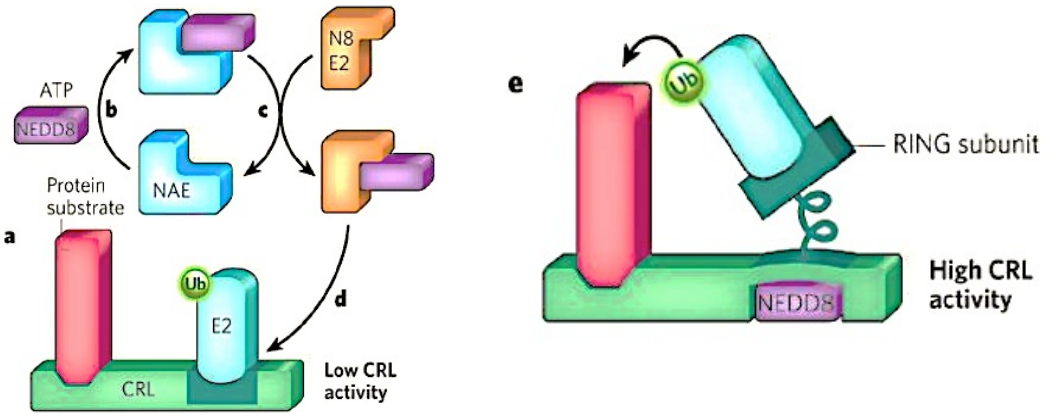

Figure 7. Representation of the CRL activation by the ubiquitin-like protein NEDD8. a) In the absence of this enzyme the CRL activity is low. b) Binding of NEDD8 to its conjugative enzyme (NAE) with ATP expends initiates the process leading to CRL activation. c) Transfer of NEDD8 to the E2 specific enzyme and then to the Cullin-ring ligase (d). e) After NEDD8 binding, a conformational changed is induced resulting in a high CRL activity by bringing the Ub-E2 complex closer to the protein substrate [30].

In *Saccharomyces cerevisiae*, the Nedd8 orthologous Rub1 (related to ubiquitin 1) promotes the neddylation of the CRL Skp1-Cdc53/cullin1-F-box [31]. Liakopoulos D., *et al* (1998) first described this ubiquitin-like protein (53% amino acid sequence similarity), in yeast, together with the enzymes required for Rub1 activation and conjugation in vivo. They concluded, based on the normal growth and phenotype of rub1 mutants, that the protein is not essential for normal cell growth and viability [32]. In the same year, Lammer D., *et al* (1998) data showed that Rub1p activation system is linked to the ubiquitin-proteasome-dependent system having the Cdc53 protein as target substrate; Rub1 is dispensable in yeast growing under standard laboratory conditions since rub1 mutant showed

normal growing rates under a wide range of temperatures. However the Rub1p pathway was found to be necessary when the function of SCF is compromised by mutations in Cdc34, Cdc4, Cdc53 and Skp1[33].

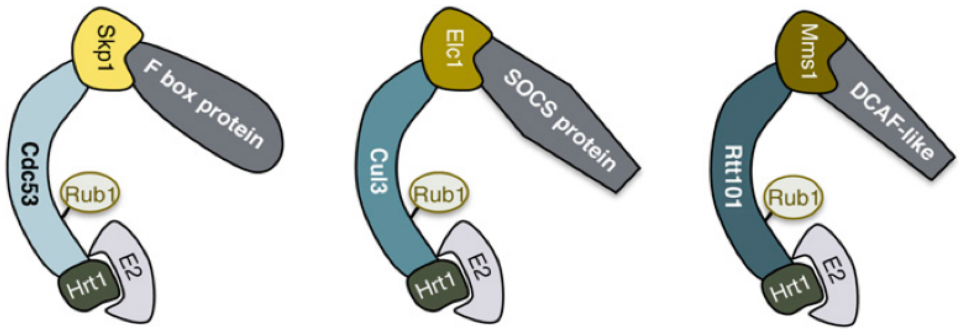

Figure 8. Classes of CRLs in S. cerevisiae: Cullins Cdc53 (cullin 1), Cul3, and Rtt101 (functionally similar to human Cul4). The C-terminal regions of cullins bind the RING protein Hrt1/Rbx1/Roc1, and the N-terminal portions interact with specific adaptor proteins (Skp1, Elc1, and Mms1), which recruit substrate receptor proteins (F-box, SOCS-box, or DCAF proteins) [34].

2.2 COP9 signalosome

The COP9 signalosome (CSN complex) was first identified in *Arabidopsis thaliana* when Wei *et al*., (1992) reported the initial characterization of a new light-regulatory locus, COP9, which mutation leads to a constitutive photomorphogenic phenotype in the absence of light [35-37].

Chamovitz D.A., *et al* (1998), proposed that this complex might also represent a novel yet conserved development regulator in both insects and mammals [35]. In insects, it was showed by Freilich S., *et al* (1999) that it plays an important part in the development of the fly *Drosophila melanogaster,* in which disruption of one or more subunits genes caused larval lethality [38]. Seeger M., *et al* (1998) identified the COP9 in mammals during a purification of proteasome from a lysate of red blood cells [39, 40] and, more recently, also in the budding yeast *Saccharomyces cerevisiae*, a CSN-like complex has been described [40, 41]. It is now clear that this complex is a key player in several cellular func-

tions such as DNA-damage response, cell-cycle control and gene expression [36, 42]. In addition, it appears to be over expressed in some human tumors due to its involvement in cell proliferation and apoptosis [43].

2.2.1 The CSN architecture

The COP9 signalosome is a conserved large multi-complex protein (450-550 kDa) with a canonical composition of eight subunits (Table 1.) that functions in the ubiquitin-proteasome pathway, regulating the activity of CRL families of ubiquitin SCF E3 complexes [36, 44].

Table 1. Comparison of the CSN subunits nomenclature in mammals, plants (*Arabidopsis*), insects (*Drosophila*) and yeast (*S. pombe* and *S. cerevisiae*). * The Csn12 subunit, in *S. cerevisiae,* its not an integrative part of the complex but interacts with it [40].

	Mammals	***Arabidopsis***	***Drosophila***	***S. pombe***	***S. cerevisiae***
CSN1	GPS1, mfh, Sgn1,	FUS6, COP11	Dch1	Caa1	CSN9
CSN2	Trip15, hAlien, Sgn2, COPS2	FUS12	Alien, Dch2		CSN10/RRI2
CSN3	Sgn3, COPS3	FUS11	Dch3		CSN11/PCI8
CSN4	Sgn4, COPS4	COP8, FUS4	Dch4		CSN12*
CSN5	Jab1, COPS5	AJH1, AJH2	Dch5		RRI1
CSN6	HVIP, Sgn6, COPS6	AtCSN6A, AtCSN6B	Dch6		CSI1
CSN7	COPS7a, Sgn7 COPS7b,	CSN7i, FUS5, CSN7ii	Dch7		RPN5/NAS5
CSN8	hCOP9, Sgn8	COP9, FUS7			

Six of the eight subunits contain a proteasome-COP9 signalosome-initiation factor 3 domain (PCI) and two of then (CSN5 and CSN6) a MPR1-PAD1-N-terminal domain

(MPN) [46]. These domains are also found in the 26S proteasome lid and in the eukaryotic translation initiation factor complex, eIF3. The degree of similarity is higher between the CSN and the lid with a direct correspondence by eight paralogous subunits while the eIF3 complex is more distinct containing a major number of subunits [45-47].

Accordingly with structural and biochemical analysis, there are two types of MPN domains: MPN^- and MPN^+/JAMM. Like was previously pointed, the second one is present in the Rpn11 subunit in the 26S proteasomal lid and it is also found in the CSN5 subunit of the CSN complex. This domain contains a metal-binding motif which carries an isopeptidase activity while the MPN^-, present in the Rpn8 lid subunit and in the CSN6 subunit of the CSN has no enzymatic activity [45]. The MPN^+/JAMM motif apparently constitutes the catalytic center for cleavage of Nedd8-cullin conjugate by CSN and of ubiquitin-substrates by the proteasome, thereby regulating the activity of CRLs [40].

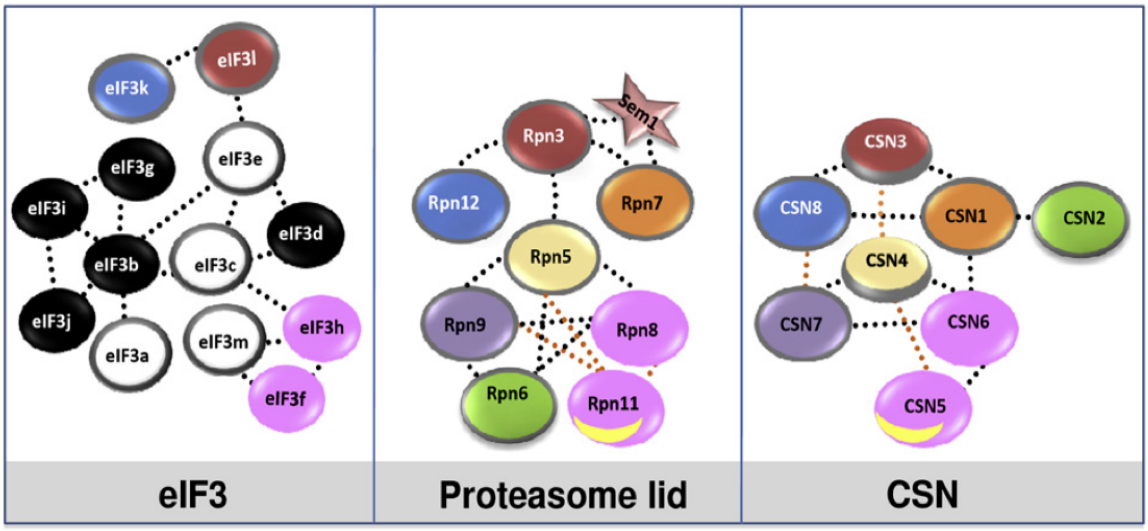

Figure 9. Schematic representation of the three complexes: eIF3, proteasome lid and CSN (left to right). PCI domains are outlined in gray while MPN subunits are pink and dashed lines show internal interactions among subunits but are not intended to accurately represent complex architecture or interaction strength. Marked with a yellow line are the active MPN+ subunits: Rpn11 in the proteasome and the CSN5 subunit in the CSN complex[45].

2.2.2 The CSN5 subunit

Among the CSN complex subunits, the CSN5 is by far the most studied subunit. This 334 residues consisting protein was first isolated as a c-Jun activation-domain-binding

protein, which stabilizes the c-Jun-DNA complex and co-activates with c-Jun transcription, and for this reason it is also named Jab1 [40,48].

The main function associated with CSN5/Jab1 is the deneddylase activity that localizes to the catalytically active metal binding MPN+/JAMM metalloprotease motif. This activity is based on the removal of the ubiquitin-like protein Nedd8/Rub1 creating neddylation/deneddylation cycles [36,44]. Besides the JAMM motif, the CSN5 possesses N-and C-terminal regions that tightly pack against the MPN fold and form an extended catalytic domain [48]. In mammalian cells, CSN5 subunit seems to be the most versatile of the CSN subunits because, apart from the other seven subunits, it can work independently and in smaller complexes. However, like Rpn11 in the 26S proteasome lid, it only manifests metalloisopeptidase activity when is part of the CSN complex and because of this it is also considered the key subunit ensuring the multiple functions of the holo-complex, [40,42].

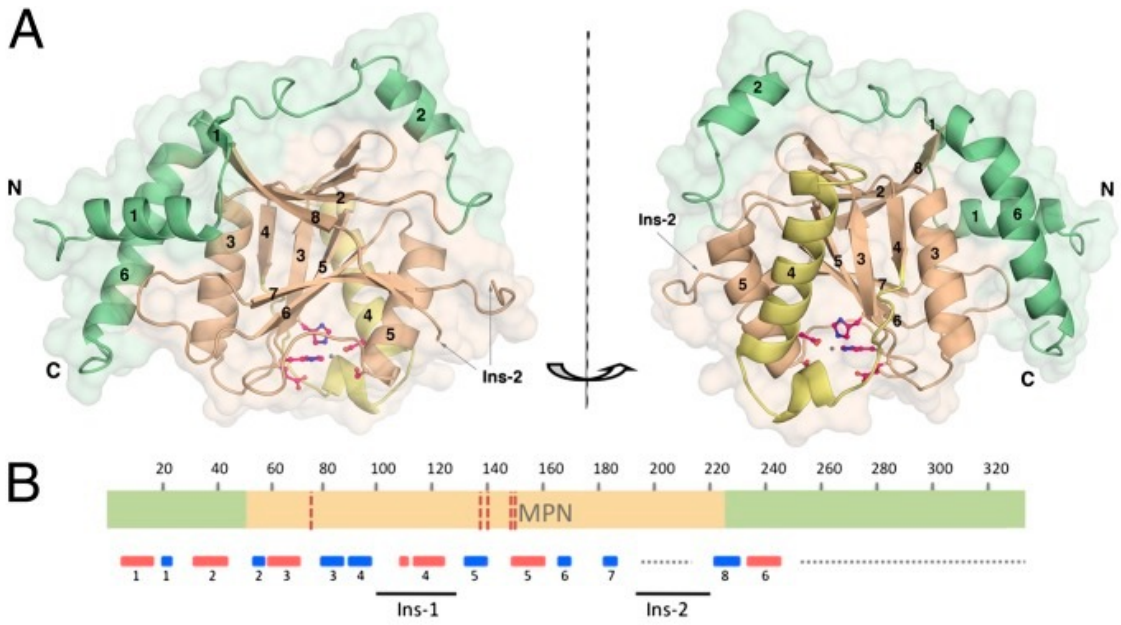

Figure 10. Overall human CSN5 comprising 1-127 residues structure and oligomeric arrangement representation, identified through mass spectrometry and N-terminal sequencing. (A) Secondary structure showing a central MPN domain in light brown and the N- and C-terminal in green. The catalytic center is show in ball-and-stick representation. (B) CSN5 domain organization. The five residues of the JAMM motif (E76, H138, H140, S148 and D151) are indicated by red dashed lines. The crystal structure was solved by selenium-single-wavelength anomalous dispersion (SAD) [48].

The versatility of CSN5 increases in each new study that is undertaken on these subunit functions and its interactions with other cellular components. Depending on the

specific target it exerts different effects on their stability. On one hand, through deneddylation activity it promotes the degradation of several factors such as p27, p53, 9-1-1 DNA repair complex, misfolded cystic fibrosis transmembrane conductance regulator (CFTR), among others (this target for destruction is possible through the already mentioned process of deneddylation of the SCF complexes [22]). On the other hand, CSN5 stabilizes several of its binding targets, including hypoxia-inducible factor 1 α subunit (HIF1-α), c-Jun and transformed mouse 3T3 cell double minute 2 (Mdm2)[46].

Cell cycle regulation involves several factors that control its progression, being crucial for a correct cell development and proliferation. A well-known factor that participates in G1 phase control progression is the cyclin-dependent kinase (Cdk)[1] inhibitor p27 ($p27^{Kip1}$) whose expression is controlled both at the level of transcription and by multiple post-translational mechanisms, among which cell cycle-dependent and substrate-specific proteolysis seems to play an important role [49]. Tomoda K., *et al* (1999) found that a specific protein encoded by the Jab1 gene interacts with this cyclin inhibitor causing its translocation from the nucleus to the cytoplasm thereby decreasing its amounts in the cell promoting a faster degradation, essential passage for cell cycle progression [50]. The two final steps of p27 down-regulation involve ubiquitination mediated by the ubiquitin ligase SCF^{Skp2} complex and proteolysis by the 26S proteasome [49,51]. So, besides its role in the p27 translocation, CSN5 is also related with its direct degradation by deneddylation of the SCF^{Skp2} complex through COP9 signalosome [43,49,50]. Deregulation of CSN5, in an overexpression context, is link to p27 protein downregulation in cancers, since one of this factor functions is to protect normal cells from undergoing abnormal cell proliferation, working as a tumor suppressor. In this way, the CSN complex can be involved in cancer development scenarios [51].

Another important factor is known to be actived under cell stress, acting in cancer prevention by maintaining the genomic integrity through cell cycle arrest and/or apoptosis. It is named p53, and like p27, is a tumor suppressor [52]. The levels of p53 in the cell are controlled by ubiquitination and consequent degradation by the proteasome allowing the maintenance of the proper functions in normal cell growth and tumorigenesis prevention. Ubiquitination of p53 is mediated by the cullin ring ligase Mdm2, which in turn is stabilized by the CSN5 subunit [51].

Tomoda K., *et al* (2004) performed studies in Jab1-null mice; they demonstrated that embryonic cells, besides lacking other CSN subunits, also showed high levels of both p27 and p53 [53].

Step by step we start to realize the great involvement of the CSN complex and particularly of the CSN5/Jab1 subunit in a large number of cell pathways, contributing to the hard task that is to keep this system on.

2.3 Yeast as model to study Proteasome and CSN complex

The eukaryotic organism currently known as the budding yeast is by far the most studied model in molecular and cell biology. Since ancient times, *Saccharomyces cerevisiae* is used in basic biotechnological process such as winemaking, baking and other types of fermentation. Nowadays this unicellular fungus is largely used in scientific research to study the expression of many important genes that have homologs in human and that are known to cause hereditary diseases [54].

The genome of this organism was totally sequenced in 1997, has about 12,06 Mbp and contains about six thousand genes organized in sixteen linear chromosomes. The functions of more than 75% of all opening-reading frames (ORFs) are known [55].

Yeast is easy to manipulate and it is possible to integrate a large spectrum of DNA molecules, like plasmid DNA by transformation, endogenous/exogenous DNA and replicative and integrative molecules by homologous recombination in a specific position of the genome. The powerful tool that is this eukaryote resides also in the ability to quickly map a phenotype-producing gene to a region of its genome and the possibility to grow in haploid and diploid state. The haploid cells could be of two genders, a or α (alpha), and to form a diploid cell, two cells of opposite mating type should mate by fusing. This allows to easily create mutants in the laboratory by promoting conjugation between two haploid cells with the desirable genotypes that then can grow and replicate by mitosis or undergo meiosis to originate four haploid cells [54].

Another important point is the fact that *S. cerevisiae* can be easily cultured because it can grow in fermentative (glucose) and non-fermentative (ethanol, glycerol) medium,

performing respiration, within a short generation time, approximately 2 hours [54,56].

As other many protein complexes, the CSN complex is essential for the development of several organisms from plants to mammals like was described before. In *S. cerevisiae* a protein complex was identified with structural and functional similarities with metazoan CSN [57]. A very interesting fact is, whereas CSN is essential for development of several different organisms such as plants (*A. thaliana*) and animals (*D. melanogaster*, *Caenorhabditis elegans*, mouse and human), *S. cerevisiae* can survive without CSN. This, together with the fact that the Csn5 subunit is highly conserved and presents a significant homology in human, makes it an interesting model to highlight the role of this multiprotein complex and its interactions with the proteasome ubiquitinase activity [44].

2.4 *Saccharomyces cerevisiae* CSN complex (ScCSN)

The *S. cerevisiae* CSN complex has a particularly divergent six subunits composition that is: Rri1, Rri2, Pci8/Csn11, Csi1, Rpn5/Nas5 and Csn9 in which only the Rri1 (Csn5 ortholog) has a MPN domain while the others have a PCI domain (See also Table.1) [58].

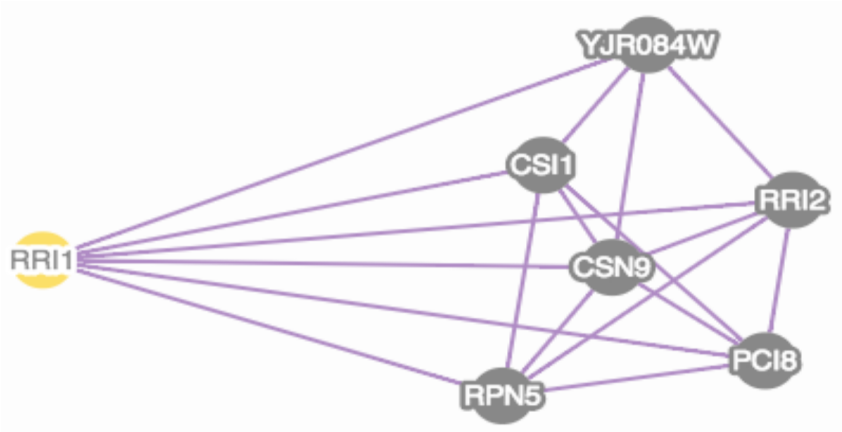

Figure 11 CSN complex subunits interactions in S. cerevisiae. In yellow is represented the RRi1 subunit (CSN5 orthololog), and in grey the other subunits. The CSN12 (YJR084W systematic name) interacts with complex but is not a constitutive subunit (see also Table 1). This scheme does not represent the tridemensional organization of the complex, just the interactions among subunits (SGD, *Saccharomyces* Genome Database).

Maytal-Kivity V., *et al* (2002) performed a study with *Sc*CSN mutants (csi1, csn5, csn9, csn12 and pci8/csn11) where they observed that, except for the csn12 mutant, there are accumulation of Rub1-modified Cdc53 confirming that, also in yeast, the CSN complex plays an important role in the activation of this E3 ligase. It also shows that, under overexpression, the extent of Rub1-hydrolase activity for all the subunits is indistinguishable from the wild-type strain, which stands for the fact that the CSN complex as a whole is necessary for the rubylation of the cullin [41]. Wee S., *et al* (2002), in their turn add human CSN to csn deficient budding yeast cell lysate, which restored, with a ratio of ~1:1 comparing with the wild-type, modified to unmodified Cdc53p, indicating an efficient removal of the Rub1p *in vitro* and, in this way, proving the existence of functional, besides structural, similarities between human and yeast CSN complex [58].

Another interesting study developed by Yu Z., *et al* (2011), points the attention in a common ScCSN and proteasome lid subunit: Rpn5. In this study they co-relate Cdc53 derubylation and proteasome integrity based in the analysis of the Cdc53-Rub1 and Cdc53 amount in ScCSN and proteasome subunit mutants and also Δrub1. They concluded that, at least in budding yeast, the CSN and proteasome are independent complexes since each one carry its own copy of Rpn5, and that CSN by itself is sufficient to perform Cul1/Cdc53 derubylation. However the authors cannot dissociate the proteasome from rubylation/derubylation cycles due to the fact that the Csn5 substrate (Rub1) shares a high structural similarity with the Rpn11 substrate (ubiquitin) and therefore, directly or indirectly, this proteasome subunit lid might influence this cycles [59].

More recently, Zemla A., *et al* (2013), showed that the carbon-source used for the metabolic activities of *Saccharomyces cerevisiae* influence the Cdc53/Cul1 derubylation response in a way that, in the presence of glucose (fermentable) the majority of the cullins is rubylated meanwhile under glycerol-growth, the rubylation is reduced, suggesting that the derubylated status is the most common and therefore the Cdc53/Cul1 is inactive in a non-fermentable medium [56].

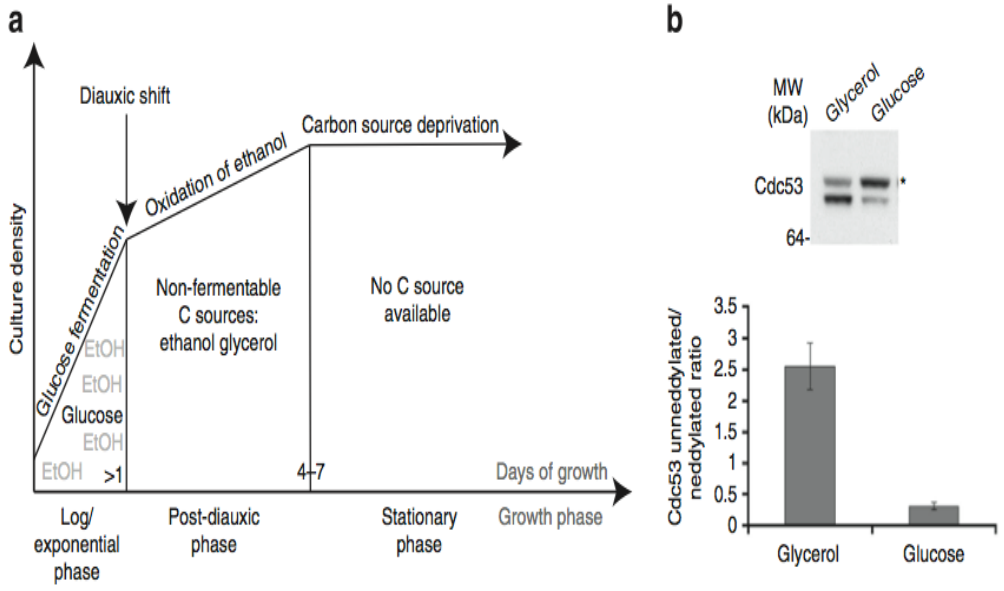

Figure 12 (a) Yeast growth curve (days of growth vs. culture density) and (b) Cdc53 derubylated/rubylated ratio in glycerol and glucose bars graphic based on the Cdc53 Western Blot. In exponential phase, yeast uses glucose as a carbon source producing ethanol. With the shift for non-fermentable carbon sources like ethanol and glycerol a diauxic shift occurs and the cells enter in a post-diauxic phase. After the exhausting of substrates, yeast goes on stationary. Concentration of rubylated cullin (*) is higher in a glucose-containing medium and consequently the ratio of derubylated/rubylated Cdc53 is higher in glycerol [56].

Besides derubylation/rubylation cycles, this protein complex (*Sc*CSN) presents other functions like interfering in the mating pheromone response or involvement in the modulation of the genes controlling amino acid and lipid metabolism [41,44].

2.5 Mitochondrion: the cell living organelle

Mitochondrion is a particular organelle, considered the powerhouse of the eukaryotic cell, contains is own DNA (mtDNA) encoding a small subset of proteins, 13 in humans and 8 in budding yeast, thus being semi-autonomous [60, 61].

The yeast, *Saccharomyces cerevisiae*, is a perfect model to study mitochondria defects since, as long as a fermentable carbon source is available, like glucose, it does not need to appeal for mitochondria because it obtains ATP as a final fermentation product [61]. For this reason it is possible to observe mitochondrial morphology defects without losing cell viability.

2.5.1 Biogenesis, structure and mitochondrial functions

In terms of structure, mitochondria have two membranes that create five different spaces: outer membrane, intermembrane space, inner membrane, inner membrane cristae and the matrix, each one having different functions [60]. Thus, mitochondrion biogenesis is a complicated process that requires a coordinated assembly and sorting of both nuclear and mitochondrial encode proteins [62].

The inner membrane is similar to the bacterial membrane in lipid constitution and it has some of the most important functions in the mitochondria metabolism. Cristae formation increases the mitochondria efficiency since it contains the proteins to perform redox of oxidative phosphorylation, NADH, succinate dehydrogenases, ATP synthases, mitochondria's fusion and fission proteins and proteins that regulate the transport of proteins and metabolites [63].

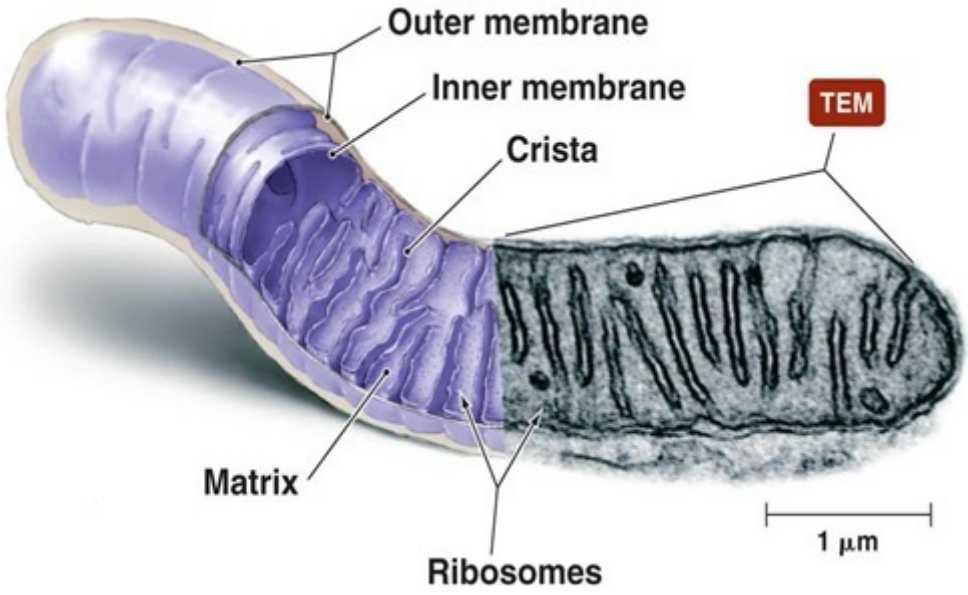

Figure 13 Mitochondria structure and organization. In the left is represented from a schematic point of view and in the right is complemented with an image made in transmission electronic microscopy.

Mitochondria grow by the incorporation of proteins, production of phospholipids and transport from others organelles, it is an essential organelle like the endoplasmic retic-

ulum, and they cannot be synthesized *de novo* by a cell. The shape, morphology, and number of the mitochondria are controlled by the balance between fusion and fission events and they are regulated by specific proteins: Mfn1, Mfn2 and OPA1 for fusion events and Fis1 and Drp1 for fission. These events have also impact on mitochondrial functions (cellular energy metabolism, survival and proliferation) and distribution in the cell [61, 63].

2.5.2 Mitochondrial inheritance and diseases

The maintenance of an intact respiratory chain is essential for life from yeast to humans. Since mitochondrion is inherited from the mother there are hereditary diseases that are linked to mutations in the mtDNA. As so is important to ensure the passage of intact mtDNA in a way that the cell will not be compromised in their respiratory capacity. However, due to the production of reactive oxygen species (ROS), the mtDNA, with aging, will inevitably be damaged by these products of the oxidative phosphorylation. [61].

S. cerevisiae reproduces by a process called budding or assymetric cell division and all the components must be divided [64]. Right after the emergence of the bud, the mitochondria are transported to the new cell through actin filaments driven by myosin motor proteins. A faithful distribution of mitochondria and mtDNA during cell division depends on many processes such as mitochondrial motility, tethering, fusion and fission and mtDNA partitioning [61].

The equilibrium between fusion and fission events is of main importance for the mitochondria viability in the cell. In yeast, after replication, cells reveal a branched tubular network around the nucleus that is frequently remodeled by this two processes [64]. If there are problems in the fission pathway, mitochondria forms interconnected nets due to continuous fusion. On contrary, if there are fusion problems mitochondria are fragmented. The proteins involved in fusion/fission equilibrium are highly conserved on evolution which recognizes the importance of mitochondria correct morphology maintenance [65]. In fact, changes in this equilibrium leads, in humans, for example, to neurodegenerative diseases. Mutation in MFN2 gene cause Charcot-Marie-Tooth (CMT) subtype 2 disease that is characterized by muscle weakness and axonal degradation of sensory and motor neurons [65]. Another well-known case is Parkinson disorder in which mutation in the Pink1 kinase

leads to neurons degeneration due to the accumulation of toxin/non-degraded proteins. This protein is targeted mainly for mitochondria because of the accumulation of ROS followed by loss of membrane potential and an increase of damaged proteins. So, lost of its function can cause alterations in mitochondria morphology due to the lack of Parkin E3 ligase recruitment that, in its turn, performs ubiquitination marking proteins for degradation by the proteasome and therefore inducing mitophagy [8, 62].

So, due to the mitochondria essential role and its susceptibility to DNA damage and production of aberrant proteins it is important that the cell possesses a quality control system able to manage this situation [1].

3. Materials and Methods

3.1 Yeast strains and growth conditions

The yeast strains can be grown in liquid or in solid media, which is supplemented with 2.15% agar (Formedium^{TM}) and placed in plates with 9 cm in diameter. Based on the conditions that we want to test, different media can be used and they can be undefined or defined changing in carbon source, growth factors and macro/micronutrients needed for the strain to grow. For an optimal growth, the cells are incubated in Yeast extract-peptone+dextrose medium (YPD), at 28ºC in agitation under aerated conditions.

Table 2. *Saccharomyces cerevisiae* strains used in this work with correspondent genotype and source.

Strain	Genotype	Source
WM-1A (W303)	MATa, his3-11, ade2-1, leu2-3,112, ura3-1, trp1-Δ2, MPR1, can1-100	Rothstein (Columbia University)
Δcsn5	MATα, his3-11, ade2-1, leu2-3,112, ura3-1, trp1-Δ2, MPR1, can1-100, YDL216c::KanMX4	EUROSCARF*
rpn11-m1	Mat a, his3Δ-200, ade2-101, leu2Δ1,ura3-52, lys2-801, trp1Δ62, bar1::HIS3	Carl Mann (CEA/Saclay, Gif-sur-Yvette, France)
Δrub1	MATα, his3-11, ade2-1, leu2-3,112, ura3-1, trp1-Δ2, MPR1, can1-100, YDR139c::KanMX4	EUROSCARF*

*EUROSCARF (European *Saccharomyces cerevisiae* Archive for Functional Analysis; Institut für Mikrobiologie, Johann Wolfgang Goethe-Universität, Frankfurt am Main, Germany)

The strains rpn11-m1/Δcsn5 and rpn11-m1/Δrub1 were obtained through mating, sporulation and tetrad dissection.

Yeast extract-peptone+dextrose medium (YPD):

- 1% yeast extract (Duchefa Biochemie), 1% bacto-peptone (Formedium^{TM}) and supplemented with 2% dextrose (Titol Chimica). Solid medium contains: 2.15% agar

Yeast extract-peptone+dextrose medium (YEP+D):

- 1% yeast extract (Duchefa Biochemie), 2% bacto-peptone (Formedium^{TM}) and supplemented with 2% dextrose (Titol Chimica). Solid medium contains: 2.15% agar

Yeast extract-peptone+glycerol medium (YPGly):

- 1% yeast extract (Duchefa Biochemie), 1% bacto-peptone (Formedium^{TM}) and supplemented with 2% glycerol (Sigma-Aldrich). Solid medium contains: 2.15% agar.

Yeast minimal media/Synthetic defined medium (SD):

- 0.17% yeast nitrogen base (without aminoacids, Difco^{TM}), 0.5% ammonium sulfate (Carlo Erra, reagents) and supplemented with 2% dextrose (Titol Chimica).

- (SD-URA): 0.17% yeast nitrogen base (with all aminoacids except uracil, Difco), 0.5% ammonium sulfate (Carlo Erra, reagents) and supplemented with 2% dextrose (Titol Chimica). Solid medium contains: 2.15% agar.

Table 3. Amino acids solution volume to make 1 L of SD medium with specific concentration in stock.

Amino acids	Stock	Concentration (ml/L)
Uracil	240mg/100 ml H_20+ 0.% (w/v) $NaHCO_3$	10
Lysine	360mg/100 ml H_20	8.3
Tryptophan	480mg/100 ml H_20	8.3
Leucine	720mg/100 ml H_20	10
Histidine	240mg/100 ml H_20	10
Adenine	500 mg/100 ml HCl (50mM)	8.3
Methionine	240 mg/100 ml H_20 (100x)	10

3.2 Bacteria strains and growth conditions

Similar to yeast, bacteria can be grown in liquid or solid media, which is supplemented with 2.15% agar (Bactoagar Difco) and placed in plates with 9 cm in diameter. In this case, the *Escherichia coli* strain was grown in *Luria-Bertani medium* supplemented with ampicillin, at 37ºC.

Table 4. *Escherichia coli* strain used in this work with the correspondent genotype and source.

Strain	Genotype	Source
DH5α	SupE44, ΔlacU169(Φ80lacZΔM15), hsdR17, recA, endA1, gyrA69thi	Miller and Mekalanos

Luria-Bertani medium (LB)

- 1% yeast extract (Duchefa Biochemie), 1% bacto-tryptone (Formedium^{TM}) and supplemented with 2% of sodium chloride (NaCl) (Formedium^{TM}). Solid medium contains: 2.15% agar.

Table 5. Antibiotic supplement for LB medium.

Antibiotic	Stock	Concentration (µg/mL)
Ampicillin (Ap)	10mg/mL	10

3.3 Plasmid vectors

The plasmids used in this work were the pRS416-GFP-Atg32 [66], kindly provided by Daniel J. Klionsky (Life Sciences Institute and Departments of Molecular, Cellular and Developmental Biology and Biological Chemistry, University of Michigan) , the plasmid expressing the GFP-Atg8 [67] that, in its turn was kindly provided by Hagain Abeliovich (Depart-

ment of Biochemistry and Food Science; Hebrew University; Rehovot, Israel) and the pVT100UmtGFP [68].

3.4 *Escherichia coli* transformation

In order to amplify the plasmids used in this work, a bacteria transformation with the *E. coli* strain DH5α was performed. The competent DH5α cells were taken from -80ºC and 100µl were transferred to an *eppendorf*. At this point, 2µl of plasmidic DNA were added and the solution left on ice for 30 minutes. A termic shock was induced by incubation for 2 minutes at 42ºC and 1 mL of LB+Amp medium was added. The cells grew for 60 minutes at 37ºC. After this, 100µl were plated in selective medium, LB+Amp, in order to have a more concentrated culture. The remaining solution was centrifuged at 4000 rpm for 10 minutes, a portion of the supernatant eliminated and the pellet ressuspend. The cells were cultured in the same selective medium, LB+Amp and placed at 37ºC to grow overnight. In this way we have 2 plates with different cell concentration.

3.5 Plasmidic DNA extraction

The extraction of the plasmidic DNA was carried with the BioRad® kit, Quantum Prep™ Plasmid Midiprep allowing us to obtain the plasmid vectors for S. *cerevisiae* transformation.

E.coli cells transformed with the plasmid vector were incubated overnight at 37ºC in 50 mL LB+Amp medium. The extraction started with a centrifugation for 20 minutes at 5000 rpm, the supernatant eliminated and the pellet ressuspend mechanically. At this point 5 mL of cell ressuspension was added and the solution vortexed followed by the addition of 5 mL of cell lysis solution with gently agitation (invert 6 to 8 times). One more centrifugation for 15 minutes at 5000 rpm and the supernatant was recuperated in a *falcon*. Meanwhile the quantum prep matrix was ressuspended and 1 mL was added to the solution in the *falcon* followed by a centrifugation for 5 minutes at 5000 rpm. After supernatant elimination, 10 mL of wash buffer was added to the pellet that was subsequently centrifuged and washed again with 600µl of the same washing buffer. The solution was then trans-

ferred to a 2 mL *eppendorf* with a spin column and centrifuged for 1 minute at 15 000 rpm being the solution that passes in the *eppendorf*, discarded. One last washing was performed with the addition of 500µl of wash buffer, centrifugation for 1 minute at 15000 rpm, elimination of the remaining in the *eppendorf* and again centrifugation in the same conditions.

The spin column was transferred to a new 2 mL *eppendorf*, 600µl of ddH_2O added and the solution centrifuged, 2 minutes at 15 000 rpm.

After extraction, the plasmidic DNA was quantified through spectrophotometry (Thermo Scientific NanoDrop™ Spectrophotometer) at the wavelength of 260nm. Protein and phenolic contamination resulting from the extraction procedure was also measured using the absorbance ratio of 260/280 and 260/230, respectively. To have "pure" DNA the ratio value should be 1.8-2.0 (A260/280) and 2.0-2.3 (A260/230).

3.5.1 Control of the extracted DNA in agarose gel

In order to verify the integrity of the plasmidic DNA extracted, an electrophoresis in agarose gel (1%) was preformed. The colorant ethidium bromide (2µl) was added after boiling the gel (40 mL TE + 0,4g agarose). The solution to load in the gel was composed by 3µl loading buffer, 2µl of DNA and 10µl of H_2O. We used the λ marker and set the conditions for 90V, approximately 45 minutes in TBE 1X running buffer. In the end of the running, the gel was exposed to UV light.

3.6 *Saccharomyces cerevisiae* transformation

Yeast cells were grown in 10 ml YPD liquid medium until reach a concentration of $5x10^6$- $2x10^7$ cells/ml (log phase). The total volume was transferred to a falcon and centrifuged for 5 minutes at 10000 rpm and the pellet resuspended with 2.5 mL of Lithium Acetate + TE 1X (Stock Lithium Acetate + TE 1X). After a second centrifugation in the same conditions the pellet was resuspended with 200 µL of Lithium Acetate + TE 1X and the volume transferred into *eppendorf* tubes.

In the *eppendorfs*, 10 µL of Salmon Sperm (previously denatured at 95ºC for 2', precisely), 5 µL of DNA and 700 µL of Solution PEG: Lithium Acetate 1X (Stock 10X) TE 1X (Stock 10X) + PEG 3350 40% (Stock 50%) were added.

The cells were then incubated for 30 minutes at 28ºC with agitation followed by another period of incubation but this time for 15 minutes at 42ºC. After, the samples were centrifuged for 1 minute at 5000 rpm, the supernatant eliminated and the pellet resuspended in the remaining solution. The transformants were plated in solid selective terrain and putted at 28ºC to grow.

3.7 Growth curve

Yeast cells were grown in 2mL of YPD liquid medium at 28ºC with agitation, until they reached a concentration of $5x10^6$- $2x10^7$ cells/ml (log phase).

To inoculate the same number of cells (10^4 cells/mL), a Burker chamber was used to calculate the cell concentration (Cells/mL= (nº of cells/12)*25*10^4*dilution) and a new inoculum was made in 10 mL YPD liquid medium and placed at 28ºC in agitation to grow. Every 2 hours, during 12 hours, the cells were counted in the Burker chamber and the concentration calculated.

After 11 hours, a second inoculum was made, under the same conditions, to reach the 14 hours of growth in the next morning.

In the second day, the first inoculum was at 25 hours and the cell concentration was calculated, for both inoculums, following the same procedure of the previous day.

3.8 Vitality test

Yeast cells were grown in 2mL of YPD liquid medium at 28ºC in agitation, until reached a concentration of $5x10^6$-$2x10^7$ cells/ml (log phase). The cell concentration was accessed by cell counting in the Burker chamber (See Growth curve protocol) and 200 cells were plated in YDP solid medium, in three replicas for each strain in study. This procedure was repeated for three times in a way of having three biological independent probes.

3.9 Stress conditions assessment

3.9.1 Temperature and carbon source

Yeast cells were grown in 2mL of YPD liquid medium at 28ºC in agitation, until reached a concentration of $5x10^6$-$2x10^7$ cells/ml (log phase). Cell concentration was calculated using the Burker chamber (See Growth curve protocol) and a dilution series was made in order to obtain the following concentrations: 10^7, 10^6, 10^5, 10^4, 10^3 cells/mL. The cells were plated in YPD and YPGly media, with a 5 µL drop to each dilution, in duplicated plates than were putted at 28ºC and 36ºC to grow overnight. In this terms we have four growth conditions: YPD 28ºC, YPD 36ºC, YPGly 28ºC and YPGly 36ºC.

3.9.2 Protein degradation, autophagy and DNA repair

Yeast cells were grown in 2mL of YPD liquid medium at 28ºC with agitation, until reach a concentration of $5x10^6$-$2x10^7$ cells/ml (log phase). Cell concentration was calculated using the Burker chamber (See Growth curve protocol) and a dilution series was made in order to obtain the following concentrations: 10^7, 10^6, 10^5, 10^4, 10^3 cells/mL.

SD solid medium with Canavanin (3 µg/mL), Rapamycin (25 nM) and 0,025% of methyl-methane-sulfonate (MMS), plus YEP+D solid medium with MMS and YPD medium with MMS at 28ºC were use to assess stress conditions in different cell concentrations as mentioned above.

3.10 Autophagy

Transformed yeast cells containing the GFP-Atg8 expressing plasmid were grown in 2 mL of YPD liquid medium at 28ºC plus 180 µL of adenine, in agitation, until reached a concentration of $5x10^6$-$2x10^7$ cells/ml (log phase). Coloration with FM4-64, for the vac-

uolar membrane, was performed and the cells observed, after a decoloration phase, at the fluorescence microscope.

3.11 Mitophagy

Transformed yeast cells containing the pRS416+GFP-Atg32 were grown in 2 mL of YPD liquid medium at 28ºC plus 180 µL of adenine, in agitation, until reached a concentration of $5x10^6$-$2x10^7$ cells/ml (log phase). In a similar way as in autophagy, the cells were colored with FM4-64, for vacuolar membrane visualization and after decoloration, were observed at the fluorescence microscope.

3.12 H_2O_2 oxidative stress

Yeast cells were grown in 3 mL of YPD liquid medium at 28ºC in agitation, until reached a concentration of $5x10^6$-$2x10^7$ cells/ml (log phase) plus 200 µL of adenine. From the culture 1 mL was taken to a new *eppendorf* and centrifuged for 1 min at 5000 rpm. The supernatant discarded and the pellet ressuspended in PBS 1X, centrifuged again (1 min, 5000 rpm) and the supernatant discarded. A mix of PBS 1X + H_2O_2 (20 mM) (20 µl of H_2O_2 (1M) + 1 mL PBS 1X) was prepared and 1 mL was added to each sample. The cells were putted at 28ºC, in agitation, in the dark for 2 hours. The cells were washed 3 times with 1 mL of PBS 1X and stained with dihydrorhodamine 123.

3.13 Microscopy (confocal and fluorescence)

3.13.1 Vacuolar phenotype: FM4-64 coloration

From the inoculum made for the autophagy and mitophagy study, a volume of 1 mL was transferred to *eppendorf* tubes with 0,6 µL of FM4-64 (*N*-(3-Triethylammoniumpropyl)-4-(6-(4-(Diethylamino)Phenyl) Hexatrienyl) Pyridinium Dibromide). At this point the coloration phase starts when the cells stay for 1 hour in agita-

tion in the dark. After this phase, the total volume is transferred to a new *eppendorf* and centrifuged for 1 minute at 5000 rpm. The cells are washed, two times, with 1 mL of YPD medium and centrifuged in the same conditions, between washes.

To end the decoloration phase, the cells were inoculated in 2 mL of YPD liquid medium for 2 hours at 28ºC with agitation in the dark. After decoloration, the cells were observed at the fluorescence microscope using Texas Red filter (excitation/emission maxima ~515/640 nm).

3.13.2 Nuclear and mitochondrial DNA: DAPI coloration

Yeast cells were grown in 2 mL of YPD liquid medium at 28ºC with agitation, until reached a concentration of $5x10^6$-$2x10^7$ cells/ml (log phase) plus 180 µL of adenine. 100 µL of cells in exponential phase were transferred to *eppendorf* tubes and 2 times of the sample's volume of formaldehyde 1% was added following 30 minutes at room temperature. The cells were centrifuged for 1 minute at 5000 rpm, the supernatant eliminated and washed with 100 µL of H_2O. After this wash they were centrifuged for 1 minute at 5000 rpm one last time and 100 µL of DAPI (4',6-diamidino-2-phenylindole) solution (1 µg/ml) prepared from the stock (1 mg/mL) was added. The cells were left at room temperature for 5 minutes and then observed at the fluorescence microscope (340/380nm excitation and 450/490nm emission).

3.13.3 Mitochondrion membrane potential: DASPMI coloration

Yeast cells were grown in 2 mL of YPD liquid medium at 28ºC with agitation, until reached a concentration of $5x10^6$-$2x10^7$ cells/ml (log phase) plus 180 µL of adenine. 100 µL of cells in exponential phase were transferred to *eppendorf* tubes, centrifuged for 1 minute at 5000 rpm, the supernatant eliminated and the pellet washed with 100 µL of H_2O. After this wash they were centrifuged for 1 minute at 5000 rpm one last time and 100 µL of DASPMI (2-(4-(dimethylamino)styryl)-1-methylpyridinium iodide) solution (1:100) prepared from the stock (0,1 M) was added. The cells were immediately observed in the fluorescence microscope (430/470 nm excitation and 545/565 nm emission).

3.13.4 ROS assay: Dihydrorhodamine 123 coloration

Yeast cells were grown in 3 mL of YPD liquid medium at 28ºC in agitation, until reach a concentration of $5x10^6$-$2x10^7$ cells/ml (log phase) plus 200 µL of adenine. From the culture, 1 mL was taken to a new *eppendorf* and centrifuged for 1 min at 5000 rpm. The supernatant discarded and the pellet ressuspended in PBS 1X, centrifuged again (1 min, 5000 rpm) and the supernatant discarded. A mix of PBS 1X + Dihydrorhodamina (1 µl for each 500 µl of PBS 1X) was prepared and 1 mL was added to each sample. The cells were putted at 28ºC, in agitation, in the dark for 2 hours and watch directly at the microscope (500 nm excitation and 536 emission).

3.14 Western blot analysis

3.14.1 Mechanical protein extraction

Yeast cells were grown in 30 mL SD (-URA) and YPD liquid media (negative control) for one day. The total cell volume was transferred to falcons and centrifuged for 10 minutes at 6000 rpm. After eliminate the supernatant, the pellet was resuspended with 500 µl of PBS 1X and the solution transferred to *eppendorf* tubes. Cells were centrifuged for 1 minute at 5000 rpm, the supernatant was eliminated till the last drop and again the pellet resuspended with a correspondent volume in lysis buffer (PBS 1X plus protease inhibitor). At this point, now considering this new volume (pellet + lysis buffer), beads (0,45 µm) were added. The samples were vortexed for 1 minute followed with 1 minute in ice; this step was repeated 5 times. A 30 minutes vortex at 4ºC was performed and the lysate recuperated in a new *eppendorf* tube. After a last centrifugation for 10 minutes at 10000 rpm at 4ºC, the supernatant was transferred to a new *eppendorf* and stored at -20ºC.

3.14.2 Protein quantification (Bradford's Method)

A solution of 10 mg/ml of BSA in lysis buffer was prepared and from this standard solution a calibration curve was made with the following concentrations: 10,5,2.5,1,0.5 and 0.25 mg/ml of BSA.

Meanwhile it was also prepared the Bradford solution (1/5 BioRad protein assay + 4/5 H_2O) considering that is necessary 1 ml for each sample that contain: 4 µl of protein extract plus 1 ml of the Bradford solution. In the case of the control, the protein extract is replaced for lysis buffer. The optical density (595 nm) was read in a spectrophotometer and the protein concentration calculated based on the calibration curve (y=ax+c).

3.14.3 Protein separation

The polyacrylamide gel was prepared in two steps: resolving gel (10%) and stacking gel (30%). For the resolving gel was added H_2O, 30% acrylamide, 1.5 M Tris (pH 8.8), 10% ammonium persulfate and TEMED (N,N,N',N'-tetramethylethylenediamine), in a total volume of 10 ml for making 1 gel. Regarding the stacking gel the composition were: H_2O, 30% acrylamide, 1.5 M Tris (pH 6.8), 10% ammonium persulfate and TEMED (N,N,N',N'-tetramethylethylenediamine), in a total volume of 5 ml for making 1 gel. The last two components must be added simultaneously and quickly because they activate each other starting the polymerization.

After the resolving gel polymerization, the stacking gel was added and in between, ethanol was used to help in the first polymerization phase by exercising weight.

To prepare the loading solution for each sample was used: Lammeli buffer 2X, a volume with a concentration of 50 µg/ml of protein previously calculated for each sample based in the Bradford´s Method plus lysis buffer. These three components were added in an *eppendorf* tube to reach a final volume of 20 µl. The solution was boiled for 5 minutes before loading the gel.

Running conditions: 80 V, 120 mA (stacking gel) and 120 V, 150 mA (resolving gel)

3.14.4 Transfer

The nitrocellulose membrane (6x8cm) was activated by passing in ethanol (10 seconds), H_2O (5 minutes) and transfer buffer (10 minutes), in agitation at room temperature. The transfer apparatus was prepared (1 sponge, 2 cardboards with 3mm, gel, membrane and again 1 sponge and 2 cardboards) and the transfer conditions were set to: 50 V and 300 mA for 1 hour and 15 minutes.

3.14.5 Revealing

After the transfer, the membrane was washed with a Blocking buffer 1X during 1h, in agitation at room temperature. Incubation with the primary antibody (anti-GFP) was took overnight in agitation at 4ºC, in a solution of 1 ml Blocking buffer 1X plus 9 ml of H_2O. The primary antibody was recovered and the membrane washed with blocking buffer for 10 minutes in agitation at room temperature; this step was repeated 3 times. The secondary antiboby (anti-rabbit) was added following a period of 2 hours in agitation at room temperature. A third phase of washing was performed, always with blocking buffer 1X during 10 minutes, with agitation at room temperature for 3 times. For last, the addition of the resolving solution (SL, chemiluminescent detection) with incubation for 3 minutes, darkling, at room temperature was the final step before the image acquisition in the Chem-iDoc™ MP imager and the treatment with the Image Lab™ software.

4. Results and Discussion

4.1 Analysis on the Δcsn5 mutant strain

4.1.1 Morphology of the Δcsn5 mutant

The *S. cerevisiae* mutant Δcsn5 was obtained from the deletion of the CSN5 gene in an isogenic *wild-type* strain (W303), as referred in the materials and methods. After observation at the optical microscope (40x), in both exponential and stationary phase, it is clear that the mutant differs from the *wild-type* in terms of size and vacuolar morphology. To confirm this, FM4-64 staining was performed and the cells observed under a fluorescence microscope before and after treatment with 0,4M NaCl to induce vacuolar fragmentation through osmotic shock (Figure 14).

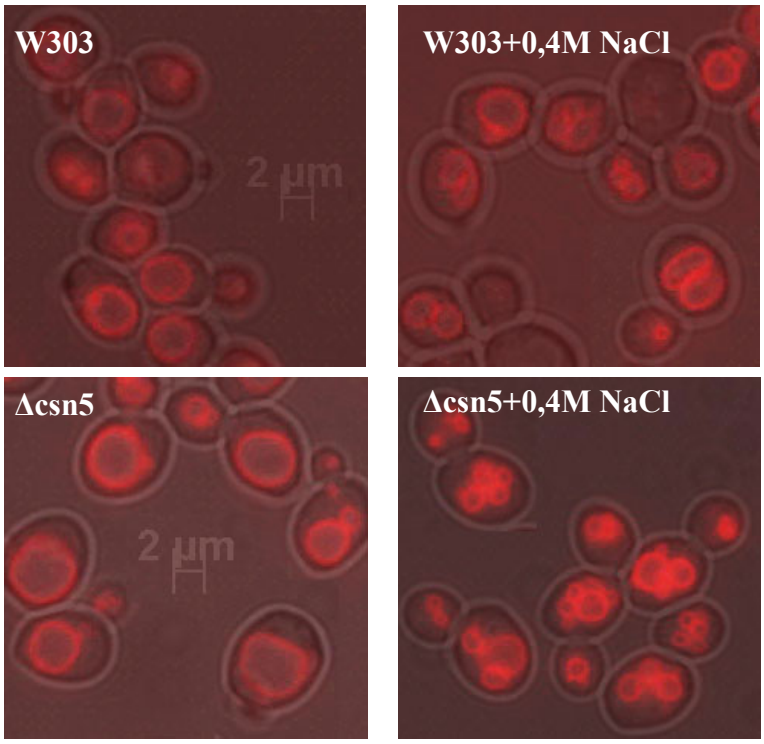

Figure 14. W303 and Δcsn5 vacuolar phenotype. The cells were grown overnight in YPD medium at 28ºC in agitation and treated with NaCl 0,4M to induce vacuolar fragmentation and stained with FM4-64. The pictures were obtained through fluorescence microscopy and scale bar is 2 µm.

The mutant Δcsn5 presents larger cells with big vacuoles, approximately 30% that occupy almost all the cell area, showing normal vacuolar fission as the WT. This means

that we do not have a biogenesis problem but instead, the vacuolar phenotype is induced by the absence of the Csn5 protein.

4.1.2 Mutant Δcsn5 growth curve

After a phenotype assessment for the Δcns5 strain it became pertinent to see the growth rate comparing with the *wild-type* strain. We know that, in the yeast *S. cerevisiae*, the duplication time is about 90 minutes in YPD medium at the optimum temperature of 28º-30ºC and that, in exponential phase (log), it achieve a cellular density of 2 x10^8 cells/ml. This log phase gives place to a post-diauxic phase after the exhaustion of glucose, which changes the cell metabolism from fermentation to respiration, a process that uses non-fermentable carbon sources such as ethanol and glycerol. When there are no carbon sources available the cells enter a stationary phase that ends with senescence state where the cell cycle is blocked in G_0 phase [54].

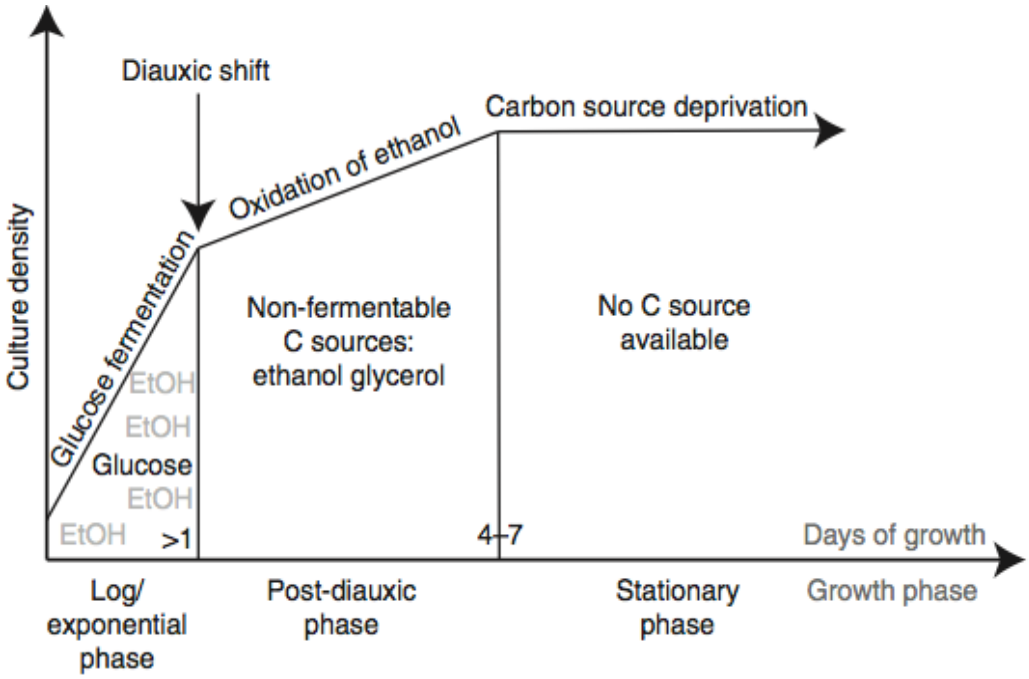

Figure 15. Saccharomyces cerevisiae growth curve (culture density vs. days of growth) [56].

From the observation of the growth curve (Figure 16) regarding the growth of our mutant strain we can see that it presents a delay in exponential phase. For example, after approximately 8 hours, the concentration is steel in the 10^4 while the *wild-type* strain is already at 10^5 cells/mL. After 20 hours both are in the stationary phase and in the shift for the post-diauxic phase (diauxic-shift) we see that the mutant strain seems to have a delay on entering in this phase, comparing with the wild-type strain. The mutant could have problems in adaption to a new carbon source during the passage from a fermentation metabolism to respiration. However, it is able to adapt and after the diauxic-shift, it equals the wild type in stationary phase.

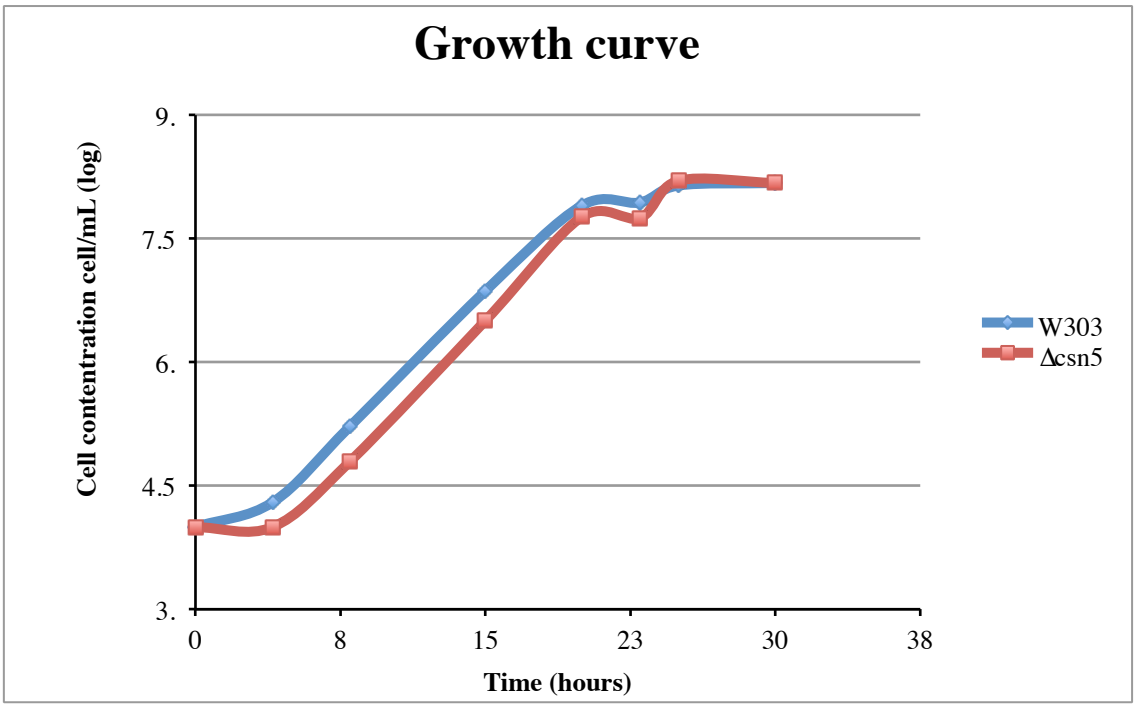

Figure 16. W303 and Δcsn5 growth curve graphic (cell concentration vs. time in hours). Cells were grown overnight in YPD medium, at 28ºC in agitation.

4.1.3 Growth test in different carbon sources

Our model organism, the yeast *Saccharomyces cerevisiae*, is a versatile eukaryote that can grow in the presence of glucose, which is its first choice for ATP production, but

cells can adapt their metabolism to non-fermentable carbon sources, which requires mitochondrial function to perform the oxidative phosphorylation for obtaining energy. When cells again encounter glucose, they rapidly switch back to fermentation.

In this line of though, and after seeing that our mutant shows a growth delay in comparison with the WT (Figure 16), we tested the growth in different carbon sources and at different temperatures: 28ºC and 36ºC.

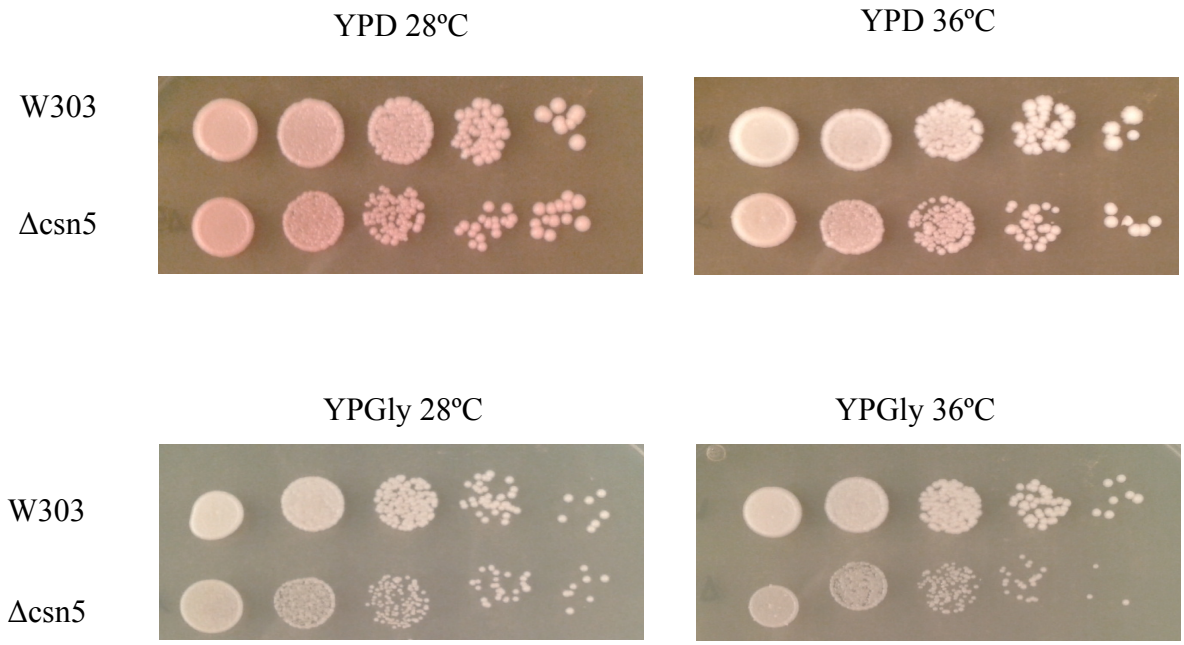

Figure 17. Serial dilutions, 10^7 cells/mL to 10^3 cells/mL spotted in glucose (YPD) and glycerol (YPGly) medium plates. The cells were grown overnight in YPD medium at 28ºC in agitation and 5 µl spot of each dilution is placed from the less diluted to the more dilute. W303 and Δcsn5 strains are first inoculated in a concentration of 10^4 cells/mL

From the analysis of the Figure 17, we see that, in YPD, Δcsn5 does not have problems in growing and is not temperature sensitive since it grows well at 28ºC and 36ºC. In YPGly medium, Δcsn5 seems to not grow so well when compared with the growth in YPD and also it shows more sensitivity at 36ºC, which can reflect mitochondrial problems.

Zemla A., *et al* (2013) demonstrated that the carbon source has influence in the Cdc53/Cul1 rubylation/derubylation being that, in YPD, most of the protein is rubylated which shows high CRL complexes activity. In the other hand, when the carbon source is glycerol, a decrease in the rubylation is observed suggesting the majority of the

Cdc53/Cul1 is inactive. The same authors showed that cells lacking Csn5 no longer derubylate the cullin after carbon switching to glycerol [56].

4.1.4 Autophagy in the Δcsn5 mutant

Unicellular organisms, such as yeast, are constantly facing environmental changes that alter the cell homeostasis and consequently activate specific responses that allow the maintenance of the intracellular equilibrium and cell survival. One of these responses is autophagy that, most of the times, is triggered in eukaryotes to overcome nutritional limitations. Autophagy induction involves the *de novo* synthesis of cytosolic double-membrane vesicles called autophagosomes that engulf parts of the cytoplasm during formation. These structures then fuse with the lysosomes/vacuoles, releasing their internal vesicles content (proteins and organelle material) which is degraded by resident hydrolases [69].

This multistep catabolic process is highly conserved in eukaryotes and in *S. cerevisiae* where have been identified approximately 30 autophagy-related (Atg) proteins. Among the Atg proteins, the ubiquitin-like protein Atg8 plays an important role in expansion of the autophagosome by mediating the number of membrane fusion events during its formation. This protein is required for both autophagy and cytoplasm-to-vacuole targeting (Cvt) pathway being the expression of the ATG8 gene increased in about 10-fold in response to starvation which causes the localization of the protein to shift from small cytoplasmic structures to the membrane of the autophagosomes in formation. During this process the Atg8p C-terminus is cleaved by the Atg4 protease resulting in the conjugation with the phosphatidylethanolamide (PE) in an ubiquitin-like reaction allowing the attachment to the autophagosome membrane [69,70]. When the complex Atg8-PE is delivered into the vacuole it is degraded by vacuolar proteases.

In this case, the study of autophagy is important to understand if the cell is suffering an early accumulation of undesired proteins. Whereas Δcsn5 presents big vacuolar phenotype, which is an indicator of autophagy, this is a plausible scenario.

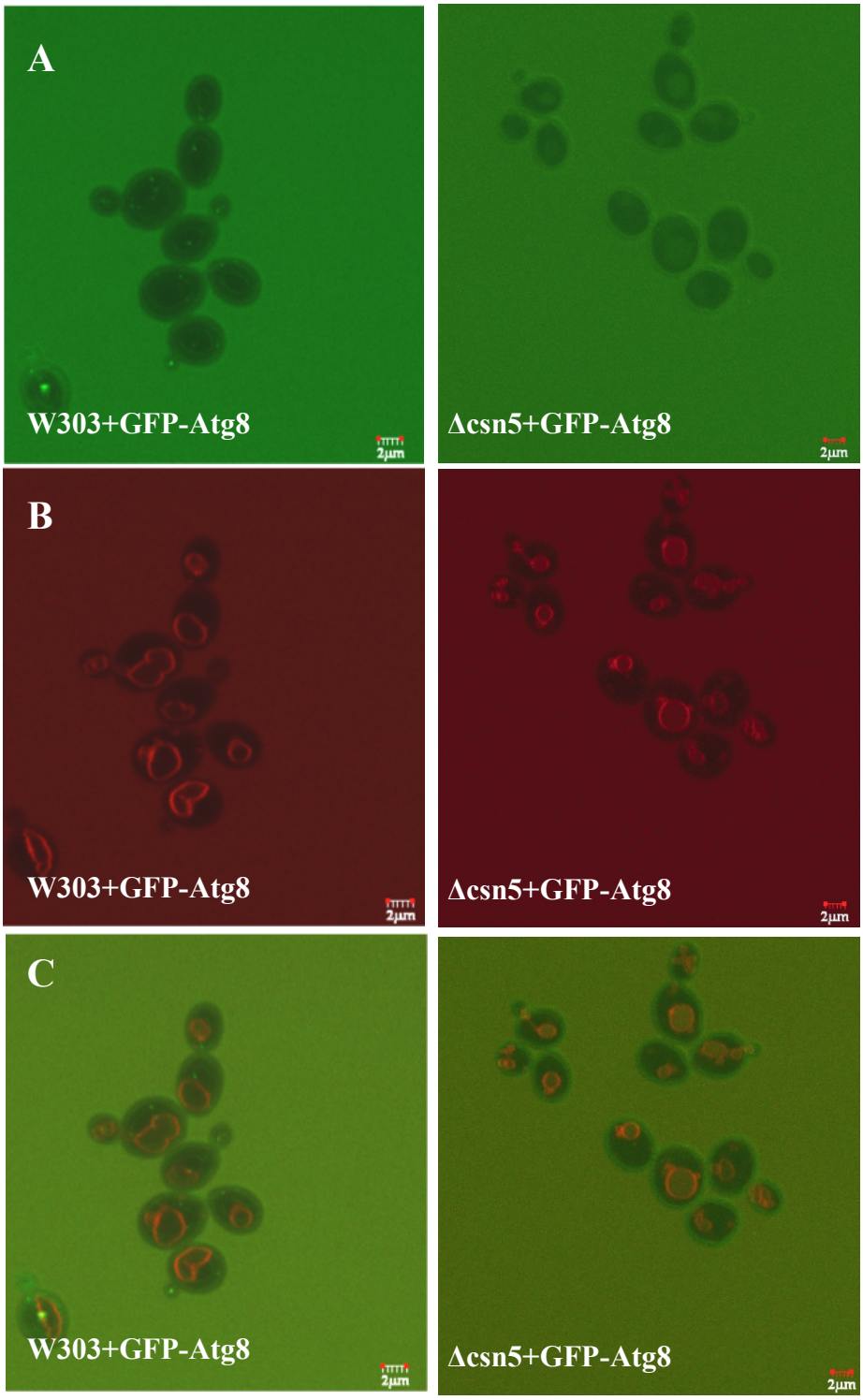

Figure 18. W303+GFP-Atg8 and Δcsn5+GFP-Atg8 images obtained through confocal microscopy, with a 2µm scale bar. The cells were grown overnight in YPD medium at 28ºC in agitation. A) Visualization of the GFP (450/490nm excitation and 500/550nm emission) in both strains. B) Vacuolar morphology evidence by FM4-64 staining. C) GFP and FM4-64 image overlay.

Therefore, for monitoring the autophagy in the Δcsn5 strain, we transformed the W303 and the mutant with a plasmid expressing the GFP, fused to the N-terminal of the ATG8, due to the fact that its behavior is the same of the Atg8 and, in this way, the autophagic process can be monitored by the vacuolar delivering and breakdown of the GFP-Atg8. This cleavage releases an intact GFP moiety, which accumulates in the vacuole as autophagy proceeds because it is relatively resistant to degradation [71].

As we can see by the observation of the Figure 18, W303 does not show autophagy in a normal growth condition while in Δcsn5 it is clear the accumulation of GFP in the vacuole. Taking in account the cell conditions: no starvation, no rapamycin treatment (inhibits the TOR complex) and exponential growth in YPD medium at permissive temperature, the autophagy induction in the mutant clearly points to defects in maintaining cell homeostasis. The autophagy complements the ubiquitin-proteasome system in mediating protein turnover [72] and perhaps due to disequilibrium in the protein waste clearance (no derubylation causes no degradation of a subset of proteasomal targeting substrates), the Δcsn5 mutant shows autophagy in exponential phase.

The vacuolar phenotype together with the sensitivity in growing in YPGly medium and an early autophagy are signs of problems on respiration and regulation of cell homeostasis.

4.2 Insights on the CSN/Ubiquitin-proteasome pathway

To better understand if there is a relation between the derubylation activity of the CSN5 subunit and the deubiquitination carried by the proteasome lid subunit Rpn11 in the ubiquitin-proteasome pathway, we performed a study regarding also the rpn11-m1 and Δrub1 single mutant strains and the double mutant strains rpn11-m1/Δcsn5 and rpn11-m1/Δrub1. The analysis passes through the cell growth assessment, maintenance and viability under different conditions of carbon source (glucose, glycerol), temperature (28, 36ºC) and inhibition (canavanin, rapamycin, MMS). This study allows an understanding of the cellular response under stress environments where DNA damage, cell cycle arrest, ROS and protein waste accumulation scenarios are present and in some cases in a greater extent triggering specific cell processes such as mitophagy.

4.2.1 Mutants growth in different carbon sources

The same study applied to the Δcsn5 was performed with the other single and double mutants in order to see if there is related sensitivity with carbon sources and/or temperature changing conditions.

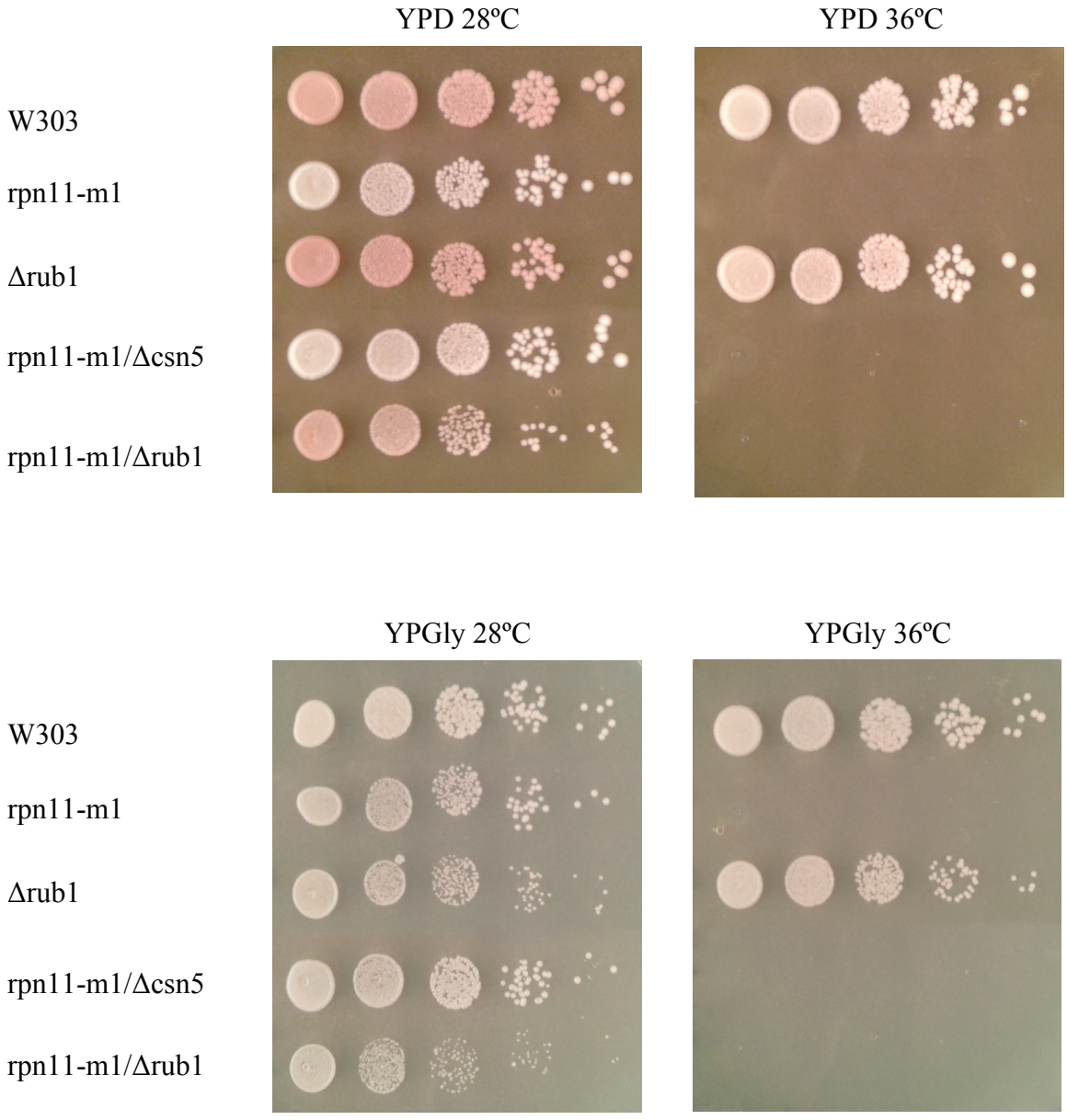

Figure 19. Serial dilutions, 10^7 cells/mL to 10^3 cells/mL spotted in glucose (YPD) and glycerol (YPGly) medium plates, at 28ºC and 36ºC. W303, rpn11-m1, Δrub1, rpn11-m1/Δcsn5 and rpn11-m1/Δrub1 strains are first inoculated in a concentration of 10^4 cells/mL. The cells were grown overnight in YPD medium at 28ºC in agitation and a 5 µl spot of each dilution is placed from the less diluted to the more dilute.

Always assuming the wild type (W303) as a control, it is clearly that rpn11-m1 is temperature sensitive not growing at the non-permissive temperature of 36ºC, in both glucose and glycerol media. As previously described (Rinaldi T., *et al* (1998); Rinaldi T., *et al* (2002)) the rpn11-m1 strain has fragmented mitochondria at permissive temperature and at non-permissive temperature it shows the characteristic phenotype of proteasome mutants such as cell cycle defects and accumulation of polyibiquitinated proteins, not degradatated due to the lack of its deubiquitinating function. So, we were already expecting the absence of growth in these conditions. This phenotype is present also in the double mutants rpn11-m1/Δcsn5 and rpn11-m1/Δrub1 that do not show growth at 36ºC, so not only the absence of the derubylation doesn't alleviate the rpn11-m1 phenotype but also the mutations show an additive negative phenotype. Moreover, the mutant rpn11-m1/Δrub1 is sensitive at permissive temperature in YPGly medium compared with the WT and single mutants rpn11-m1 and Δrub1.

4.2.2 Growth curve

The construction of the growth curve provides us a general overlook on the strains growth until they reach a stationary phase in glucose rich medium. Through Figure 20 observation we see that among the single mutants, Δcsn5 is the one that has the slowest grow, interestingly accompanied by the double mutant rpn11-m1/Δrub1, which confirms the data showed in the analysis of the growth in different carbon sources. Regarding the other double mutant rpn11-m1/Δcsn5 shows a normal growth together with the other two single mutants reaching first the concentration of 10^8 cells/mL. So, we can conclude that the rpn11-m1/Δrub1 has the slowest growth and even after 30 hours it stays in the concentration of 10^7 cells/mL. The same behavior was expected regarding the rpn11-m1/Δcsn5 strain, due to the slowest Δcsn5 growth comparing with the WT and also because the conditions of the rpn11-m1/Δrub1 and rpn11-m1/Δcsn5 cells are the same respecting the defect in maintain the natural functioning of the rubylation/derubylation cycles. This result leads to think that this mutant can be a revertant.

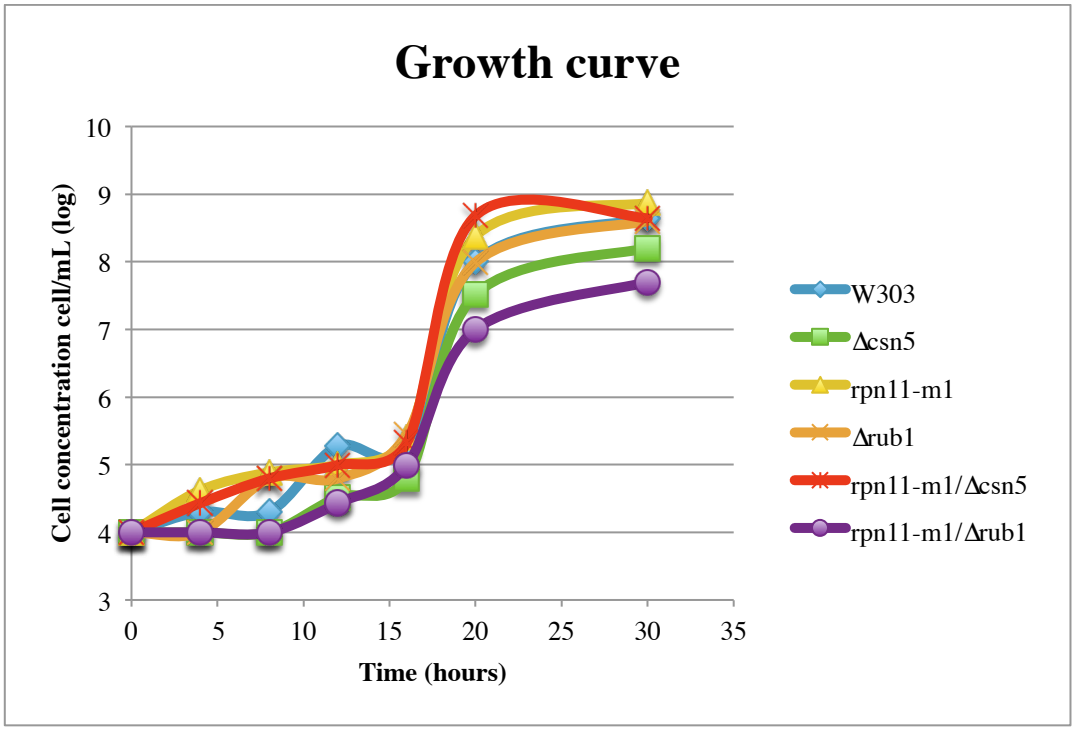

Figure 20. Wild-type (W303), single mutants (Δcsn5, rpn11-m1, Δrub1) and double mutants (rpn11-m1/Δcsn5, rpn11-m1/Δrub1) growth curve graphic. Cells were grown in YPD medium, overnight at 28ºC in agitation.

4.2.3 Vitality assessment

Taking into account the results of the growth curve it should be interesting to verify if, in fact, the double mutant rpn11-m1/Δrub1 has growth problems in YPD medium at the permissive temperature of 28ºC. What was found in the vitality test confirms the results obtained in the growth curve: the double mutant has a low percentage of living cells even when comparing with the other mutants. This can be observed in the Figure 21 of the normalized percentage of vitality where rpn11-m1/Δrub1 has about 27% vitality, which means that, in 200 cells only 54 grew to form a colony, while the other strains have more than 50% of vitality. Regarding rpn11-m1/Δcsn5 it has a vitality of around 60%, higher than rpn11-m1 that presents a vitality of 52% (See Appendix 2.1). Although it is in concordance with the growth curve we were expecting that the double mutant rpn11-m1/Δcsn5 had a cell vitality closer to the rpn11-m1/Δrub1, like it was also said before in the analysis of the curve. These results show a cumulative defect carried by the mutations that leads to a de-

crease of cellular viability since the rpn11-m1/Δrub1 have a low percentage of cells growing in the conditions considered ideal (Glucose-rich medium, 28ºC) when compared with the single mutants, Δcsn5, rpn11-m1 and Δrub1.

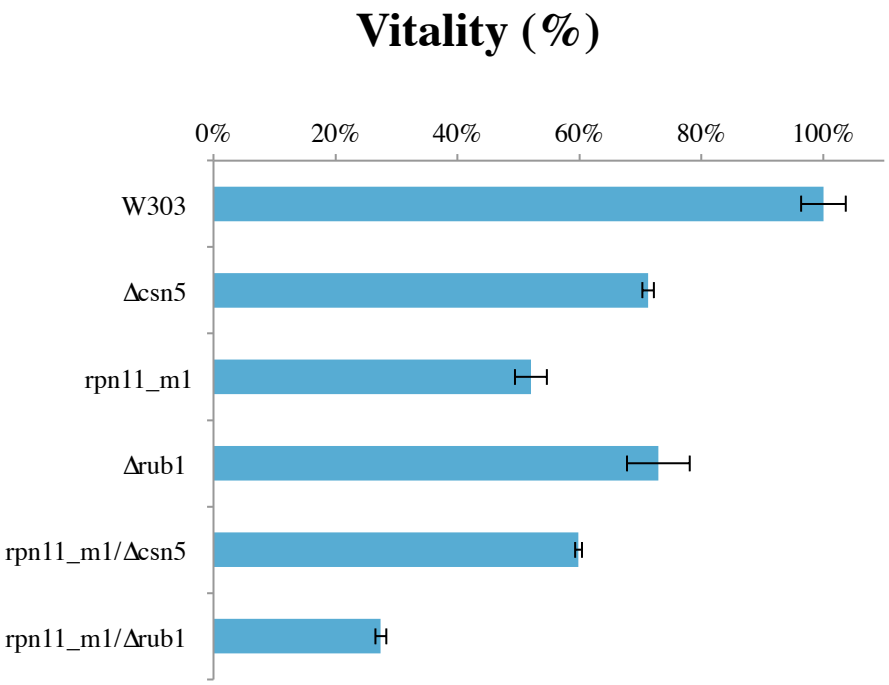

Figure 21. Wild-type (W303), single mutants (Δcsn5, rpn11-m1, Δrub1) and double mutants (rpn11-m1/Δcsn5, rpn11-m1/Δrub1) vitality (%) graphic. Cells were grown overnight in YPD solid medium at 28ºC. Values are mean ± standard deviation from three experiments (α=0.05).

4.2.4 DNA stability

With the aim of understand if the DNA stability is compromised we visualized the DNA staining of the cells with DAPI, a dye that intercalates in the A-T bond in live cells, after they grew overnight at 28ºC and after a shift to the non-permissive temperature of 36ºC during 5 hours.

The post-translational modifier ubiquitin, like the name indicates, is ubiquitous in the cell and because of that it virtually control every aspect of the cellular metabolism, in-

cluding the promotion of DNA transcription by ensuring proteasome-mediated turnover of short-living transcription factors [73]. E3 ligases and DUBs are linked to several aspects of DNA transcription regulation and damage responses, which are in agreement with the role-played by ubiquitin in chromatin compaction and decompaction through histone tail ubiquitination. As we know the level of chromatin compression affects the accessibility of the transcription factors to the DNA therefore regulating gene expression and also the possibility of initiate DNA repair by ensuring access to the lesion [73,74].

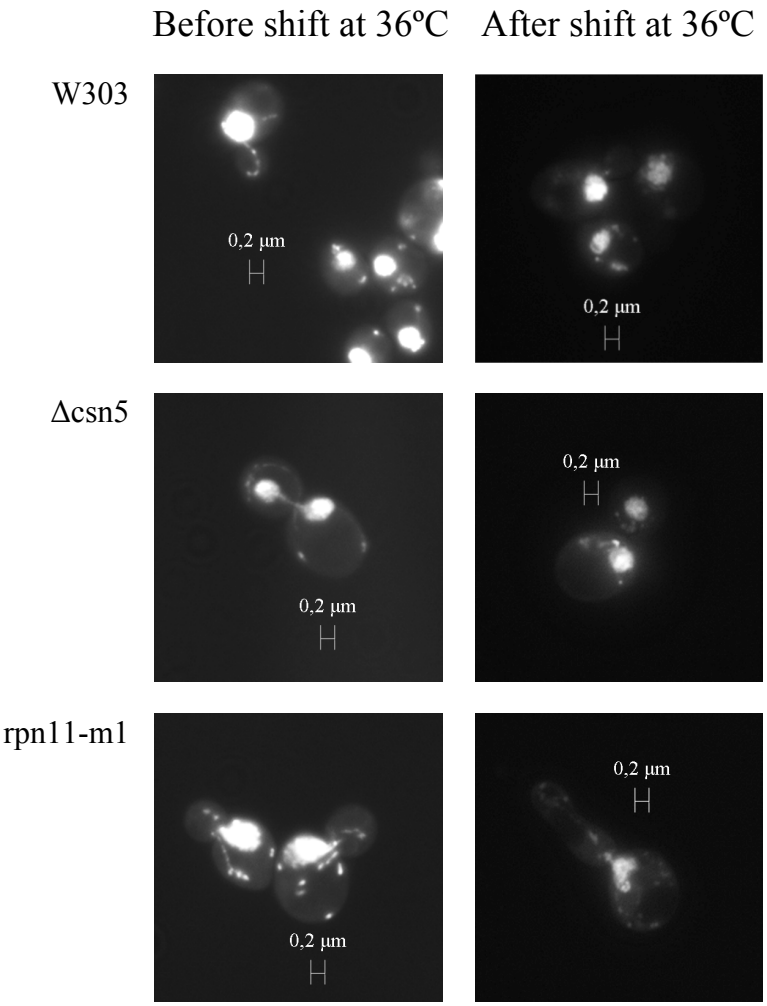

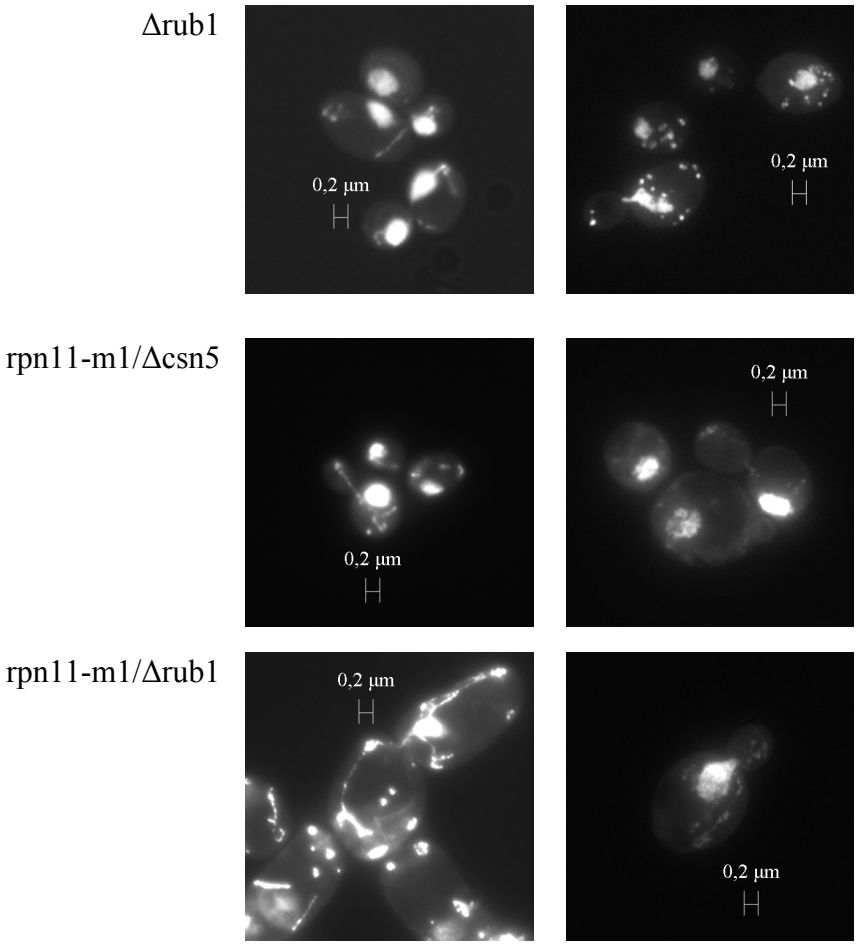

Figure 22. Fluorescence microscope obtained pictures of WT, single mutants (Δcsn5, rpn11-m1, Δrub1) and double mutants (rpn11-m1/Δcsn5 and rpn11-m1/Δrub1) strains grew in glucose rich medium (YPD) at 28ºC overnight in agitation and after shift to 36ºC for 5 hours from the initial culture at 28ºC. DAPI coloration was applied and the scale bar is 0,2 μm to all the pictures.

From the observation of the pictures obtained through fluorescence microscopy (Figure 22) we see, first of all, the aberrant cell morphology of the double mutant rpn11-m1/Δrub1.

The double mutant rpn11-m1/Δcsn5 immediately after the construction of the strain was very similar to the rpn11-m1/Δrub1 phenotype, while in this experiment the rpn11-m1/Δcsn5 mutant is accompanied only by increase in cell size after the shift to 36ºC. Even if we maintained the strain to -70°C, maybe the rpn11-m1/Δcsn5 has reverted and we are reconstructing it again. However, we can still see an aberrant nuclear morphology at 36°C in both the two double mutants: the nucleus is not compact, a phenotype already observed for rpn11-m1. After the shift to 36ºC its clear a decompression of the nuclear DNA that

could indicate lost of chromatin structure and in the case of the rpn11-m1 mutant is accompained by the presence of elongated cells due to cell cycle arrest. The mutant Δcsn5 shows the same decompression of both nuclear and mtDNA while Δrub1 shows no problems.

Concerning the mitochondrial DNA, it is visualized in all strains as dots, which correspond to nucleoids (mitochondrial DNA compacted with proteins).

4.2.5 Mitochondrial membrane potential ($\Delta\Psi_m$)

Along with the observation of alterations in DNA morphology it was also analyzed the mitochondrion membrane potential.

DASPMI is a dye that informs us about the membrane potential in the mitochondria since it localizes in the inner membrane where the transport of hydrogen protons creates differences in the quantity of positive charges that are present inside and outside the membrane therefore creating what is call the membrane potential [75].

Besides being the center of the cell energy production, mitochondrion also intervenes in other processes for normal cell functioning like cell calcium signaling, regulation of the cell redox state, transport of metabolites, etc. But one of the most important roles is the regulation of the cell life-death transition and the measure of the membrane potential give us an insight on this issue. Energy production and alterations on the mitochondrion membrane potential is related since its maintenance is crucial for ATP synthesis.

In a balancing physiologic state, the membrane potential is negative due to the gradient of protons that flows through the mitochondrion inner membrane by active transport, process that allows the energy production in the F_0/F_1 ATP-synthase (Complex V) thus completing the electron transport chain (ETC).

During cellular stress the $\Delta\Psi_m$ is altered and consequently the concentration of intracellular ionic charge change leading to alterations in ATP production [76,77].

The tubular morphology that characterizes the mitochondria is important in order to keep their functions and ensure their survival through fusion and fission events. Also, this organelle does not work alone in the cell, for example it communicates with the endoplasmic reticulum in metabolites exchange and therefore its tubular distribution allows all this processes

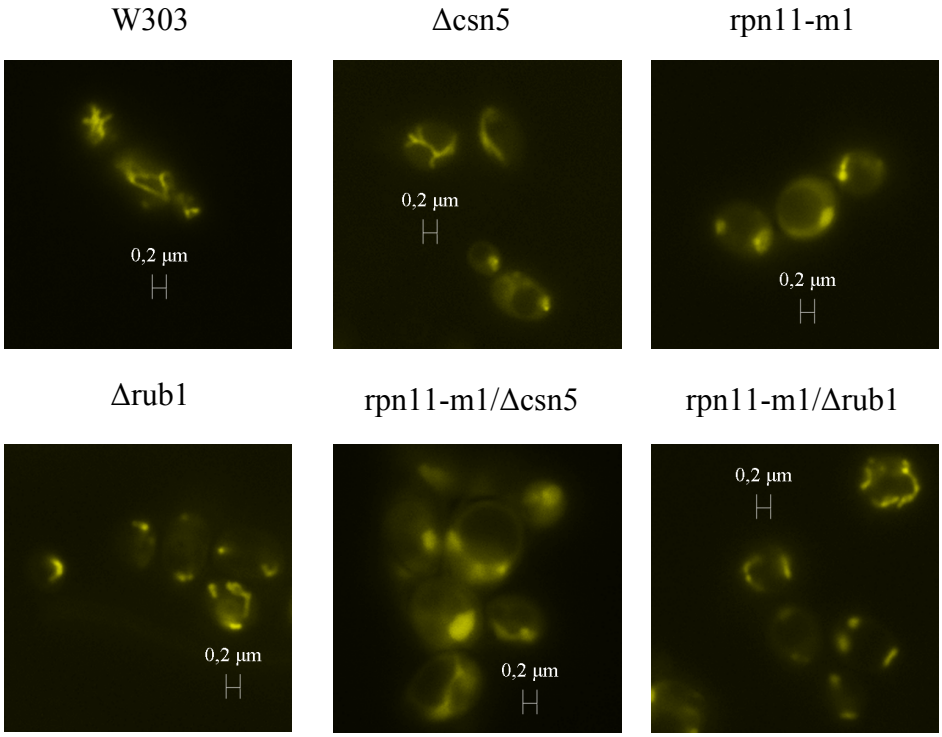

Figure 23. Fluorescence microscope obtained pictures of WT, single mutants (Δcsn5, rpn11-m1, Δrub1) and double mutants (rpn11-m1/Δcsn5 and rpn11-m1/Δrub1) strains grew in glucose rich medium (YPD) at 28ºC overnight and stained with DASPMI. The scale bar is 0,2 μm to all the pictures.

Through the observation of the Figure 23, we see in the wild type strain, a functional mitochondria with its characteristic reticular form that distinguishes it from other organelles. However, the single mutant rpn11-m1 reveals fragmented but functional mitochondria since they are stained by the DASPMI dye informing for the presence of an active membrane potential. When we have a decrease of mitochondria potential, the dye remains in the cytoplasm. With the exception of the WT and Δrub1 strains, all the mutants, Δcsn5, rpn11-m1, rpn11-m1/Δcsn5 and rpn11-m1/Δrub1 show abnormal fragmented mitochondria, indicating an involvement of rubylation in maintaining the mitochondrial morphology.

Following these results, and already knowing that rpn11-m1 and the double mutants have fragmented mitochondria, we decided to focus our attention in Δcsn5 and Δrub1 mutant strains directly correlated with the rubylation/derubylation cycles. For this we observed the mitochondrial membrane potential in exponential, early stationary and late sta-

tionary phase, as well as the mitochondrial morphology (See sub-subchapter 4.2.6) in the same conditions.

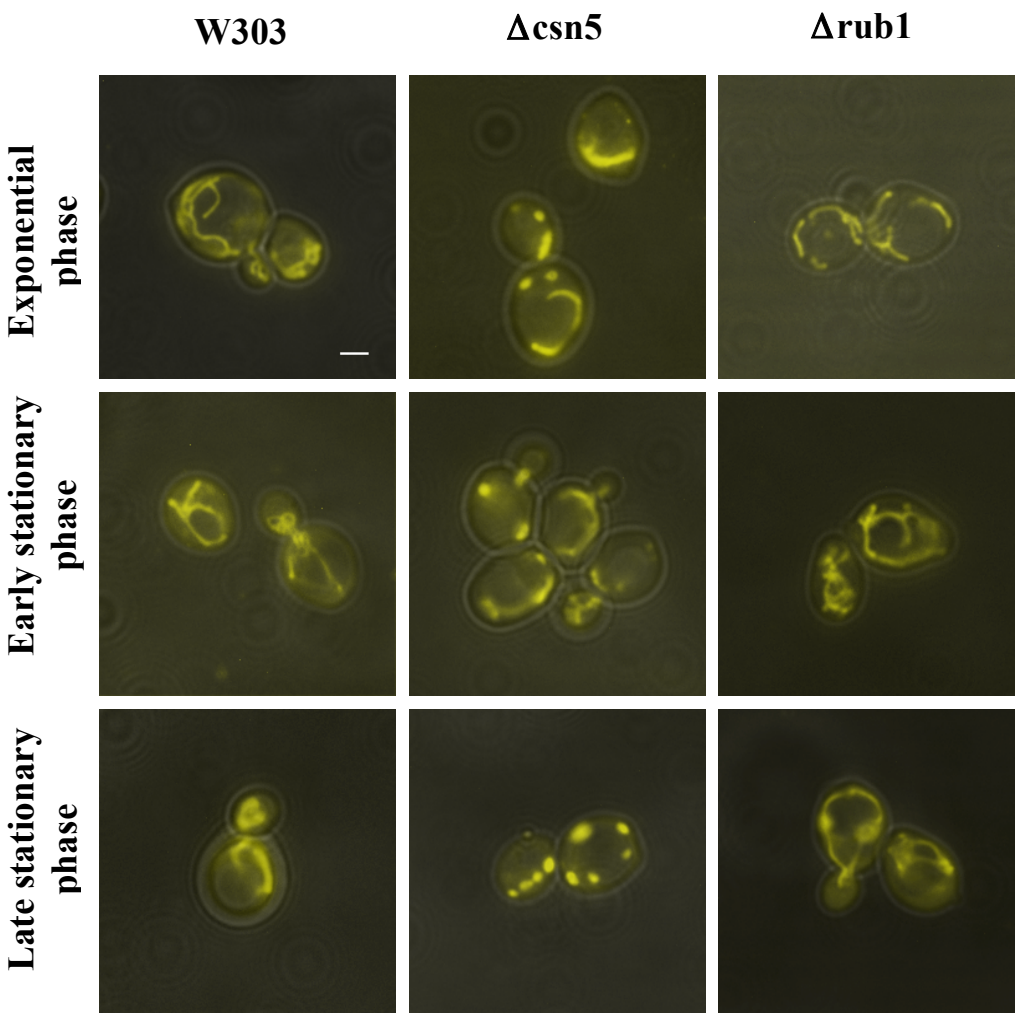

Figure 24. Fluorescence microscope obtained pictures of WT, Δcsn5 and Δrub1 in exponential, early stationary and late stationary phase. Strains grew in glucose rich medium (YPD) at 28ºC overnight and stained with DASPMI. The scale bar is 0,2 μm to all the pictures.

In this analysis we clearly see that Δcsn5 as a functional but fragmented mitochondria compared with the WT and Δrub1 (Figure 24) that shows no problems, even in late stationary phase. The Δcsn5 starts showing mitochondrial defects already in exponential phase where we see that the mitochondria tubular structure is not as clear as in WT and Δrub1. When arrives at late stationary phase, the fragmentation is evident, while Δrub1 conserves the tubular structure revealing no problems in maintain the intrinsic mitochondrion dynamics.

4.2.6 Mitochondrial morphology

To study the mitochondrial morphology along with the membrane potential we transformed the strains (WT, Δcsn5 and Δrub1) with a plasmid expressing a mitochondria-targeted GFP, that encodes for a fusion protein comprising the mitochondrial processing peptidase (MPP). This mitochondrial enzyme is located in the matrix of the organelle, in fungi and mammals [68].

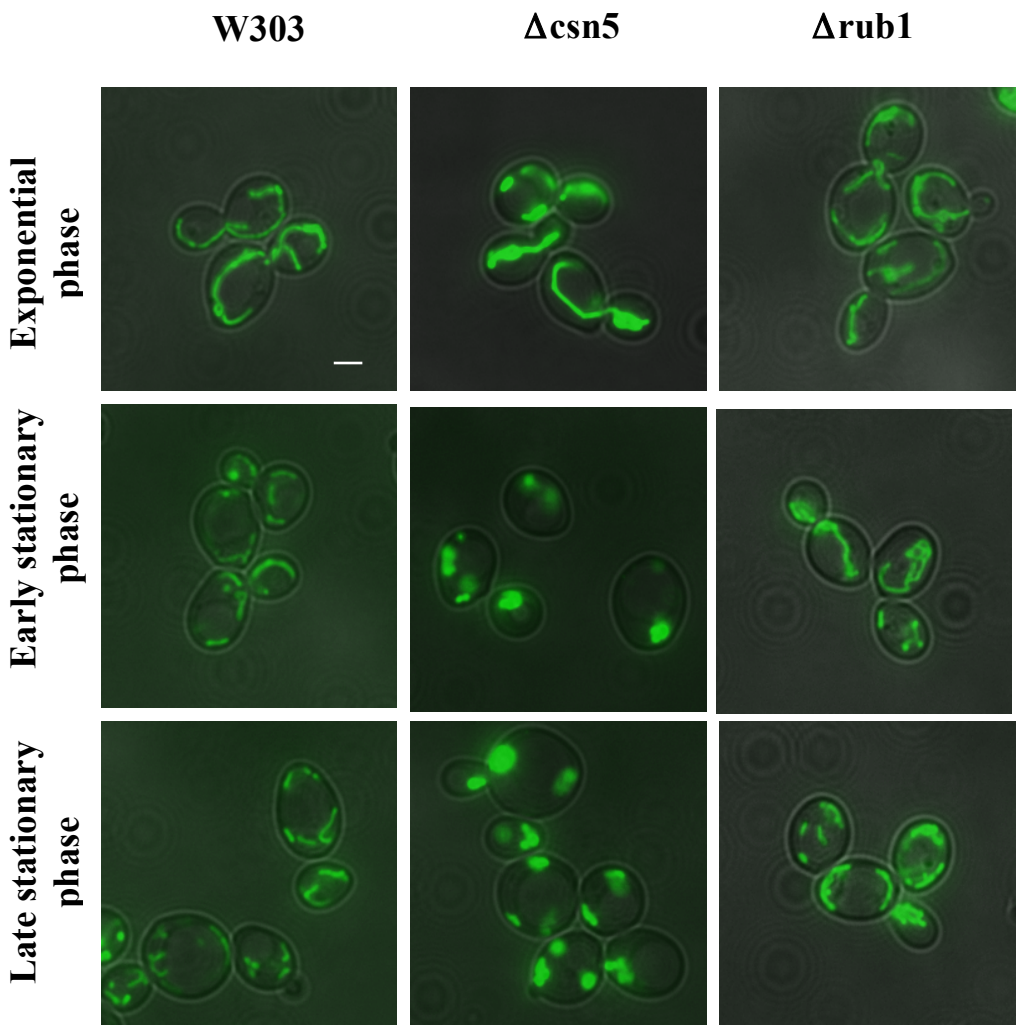

Figure 25. Fluorescence microscope obtained pictures of WT, Δcsn5 and Δrub1 transformed with the mtGFP (pVT100UmtGFP) in exponential, early stationary and late stationary phase. Strains grew in glucose rich medium (YPD) at 28ºC, overnight in agitation. The scale bar is 0,2 μm to all the pictures.

From the analysis of the Figure 25 we see that, Δcsn5, when enters in stationary phase, the mitochondrion morphology alters and we see fragmentated mitochondria. However, already in exponential phase, if we compare with the WT and Δrub1, it is interesting to see that Δcsn5 has mitochondrial defects whereas Δrub1 maintains the tubular characteristic morphology. This shows that, in the regulation of the cullin, the role played by the Csn5 subunit in the rubylation/derubylation cycles is critical for a correct mitochondrion function.

4.2.7 Genotoxic and proteotoxic stress

In order to evaluate the response to agents causing DNA damage and protein instability, wild type and mutant strains were subjected to the presence of the alkylating agent methyl methanosulfonate (MMS), 0.025% concentrated in YEP+D, YPD and SD medium plates, the amino acid canavanine in a concentration of 3 μg/mL and rapamycin (25nM) both in SD medium plates, at permissive temperature (28ºC) for 3 days and 5 days with YPD medium as a control.

MMS is a DNA damaging agent known to induce mutagenesis and recombination events through methylation of both guanine (to 7-methylguanine) and adenine (to 3-methyladenine). This modifications cause base mispairing and replication blocks therefore stopping the cell cycle [78]. Ben-Aroya S., *et al* (2010) link for the first time, the double strand break repair mechanism with the nuclear proteasomal activity. They did a systematic screen of a collection of temperature sensitive alleles (Ts) on yeast and revealed that proteasomal subunits represent a major functional group with an evolutionary conserved role in chromosome instability . In this study, DNA damaged was induced with 0.025% MMS in YEP medium. For this reason we decided to test our mutants in the same condition and compare with the conditions used in the laboratory, YPD and SD media.

The amino acid canavanine, in its turn, is an arginine analog that can be efficiently incorporated into nascent proteins, thereby producing structurally aberrant proteins that may not function properly [79].

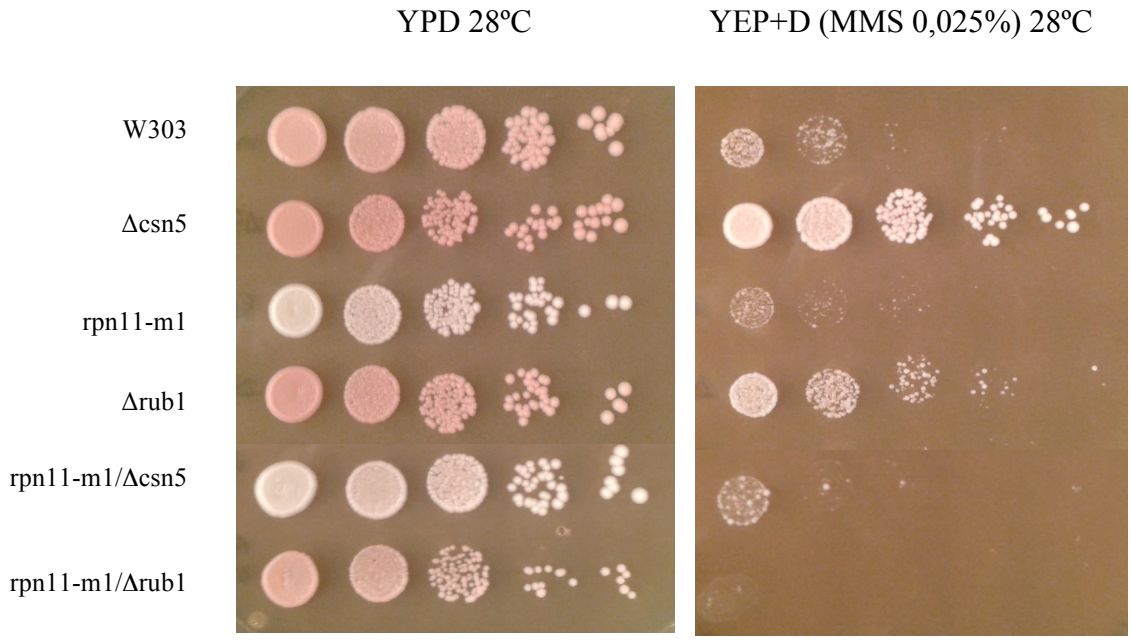

Figure 26. Serial dilutions, 10^7 cells/mL to 10^3 cells/mL spotted in YPD, YEP+D (MMS 0,025%), at 28ºC. W303, rpn11-m1, Δrub1, rpn11-m1/Δcsn5 and rpn11-m1/Δrub1 strains are first inoculated in a concentration of 10^4 cells/mL. The cells were grown overnight in YPD medium at 28ºC in agitation and a 5 µl spot of each dilution is placed from the less diluted to the more dilute.

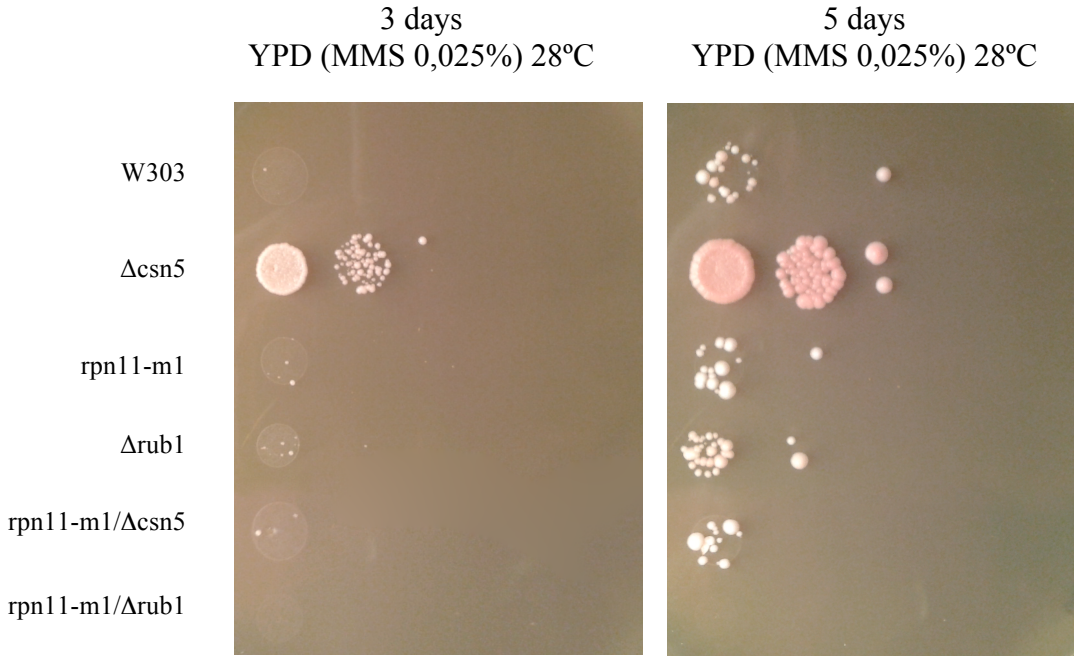

Figure 27. Serial dilutions, 10^7 cells/mL to 10^3 cells/mL spotted in YDP (MMS 0,025%) medium plates, at 28ºC, after 3 and 5 days of growth. W303, rpn11-m1, Δrub1, rpn11-m1/Δcsn5 and rpn11-m1/Δrub1 strains are first inoculated in a concentration of 10^4 cells/mL. The cells were grown overnight in YPD medium at 28ºC in agitation and a 5 µl spot of each dilution is placed from the less diluted to the more dilute.

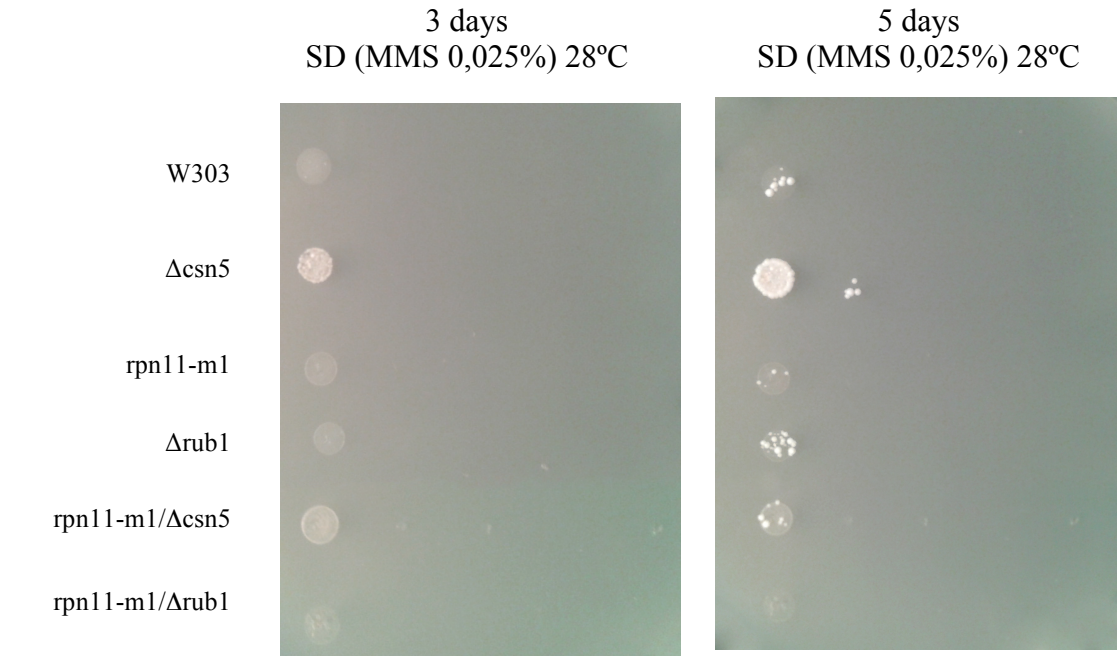

Figure 28. Serial dilutions, 10^7 cells/mL to 10^3 cells/mL spotted in SD (MMS 0,025%) medium plates, at 28ºC, after 3 and 5 days of growth. W303, rpn11-m1, Δrub1, rpn11-m1/Δcsn5 and rpn11-m1/Δrub1 strains are first inoculated in a concentration of 10^4 cells/mL The cells were grown overnight in YPD medium at 28ºC in agitation and a 5 µl spot of each dilution is placed from the less diluted to the more dilute.

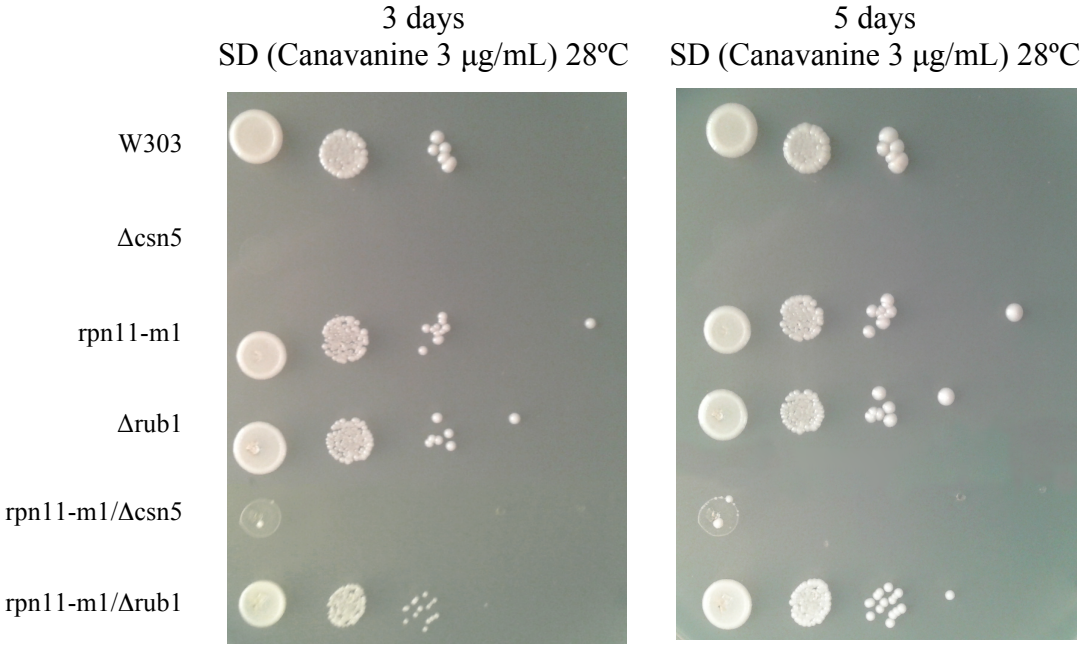

Figure 29. Serial dilutions, 10^7 cells/mL to 10^3 cells/mL spotted in SD(Canavanine 3µg/mL) medium plates, at 28ºC, after 3 and 5 days of growth. W303, rpn11-m1, Δrub1, rpn11-m1/Δcsn5 and rpn11-m1/Δrub1 strains are first inoculated in a concentration of 10^4 cells/mL The cells were grown overnight in YPD medium at 28ºC in agitation and a 5 µl spot of each dilution is placed from the less diluted to the more dilute.

Analyzing the obtained results (Figure 26, 27, 28, 29) we see that the Δcsn5 and rpn11-m1 mutants have an opposite behavior since the first is resistant to MMS and sensitive to canavanine and the second is sensitive to MMS and resistant to canavanine. In its turn, Δrub1 shows resistance to both while rpn11-m1/Δcsn5 is sensitive to both conditions and rpn11-m1/Δrub1 is just resistant to canavanine (Figure 29).

The action of damaging DNA agents like MMS causes cell cycle delay due to checkpoint activation, a necessary pathway that allows DNA repair and cell cycle progression in conditions of genetic stability. Checkpoints redundancy guarantees the success of this control mechanism that is regulated by multiple enzymes such as Rad27, Rad24, Mec3, Rad17, Sgs1, among others. The degradation of these enzymes is a crucial step for cell cycle progression and it is done via ubiquitin-proteasome [80]. Besides, it is also known that mutations in the CDC53 gene can cause cell cycle arrest in yeast, which might be related with the targeting for degradation by the proteasome of some of the proteins involved in the checkpoint control [81] . However, recently, Karpov D.S., *et al* (2013) showed that proteasome inhibition enhances resistance to DNA damage via upregulation of Rpn4-dependent DNA repair genes. RPN4 is a transcriptional factor that stimulates the expression of proteasome genes and also genes involved in the response to DNA damage, which deletion sensitizes yeast to various stress conditions. The point is that the Rpn4 is a short-life protein being rapidly degraded by the proteasome creating a negative feedback. So, considering the scenario described by Karpov D.S., *et al* (2013) stabilization of Rpn4 protein can lead to an upregulation of Rpn4-dependent DNA repair genes and therefore creating a resistance to DNA damage agents. However, there is always the other side of the coin, where the consequent accumulation of proteins due this upregulation can cause a proteotoxic effect on the cell and that's the reason why there are controversial opinions on this subject [71].

Regarding these findings and the obtained results, Csn5 could be related with the Rpn4 degradation, for example this protein could be a substrate for the Cdc53 ligase, and in Δcsn5 and Δrub1 scenarios its degradation is compromised leading to an increased resistance to MMS. In the other hand, the proteasome mutant rpn11-m1 is sensitive, revealing a high complex regulation system in which the balance between overexpression and degradation is tightly controlled. Consequently, rpn11-m1/Δcsn5 and rpn11-m1/Δrub1 are also sensitive which shows us the importance of an active proteasome activity in these conditions.

In the Δcsn5 strain it is observed a high sensitivity to canavanine, which show us that, the Csn5 subunit plays in fact an important role in the cell capacity to degraded non-functional proteins. Interestingly, the Δrub1 is not sensitive to canavanine showing that the function of the Csn5 is more relevant for the correct protein degradation than the function carried by the Rub1 protein.

In its turn, rapamycin is an antibiotic whose target is the central component of the TOR (target of rapamycin) pathway, the TOR kinase, through binding to a cytosolic immunophilin termed FK-binding protein (FKBP-12). This serine/threonine protein regulates cell growth, cell proliferation, motility and survival, protein synthesis and transcription [84,85].

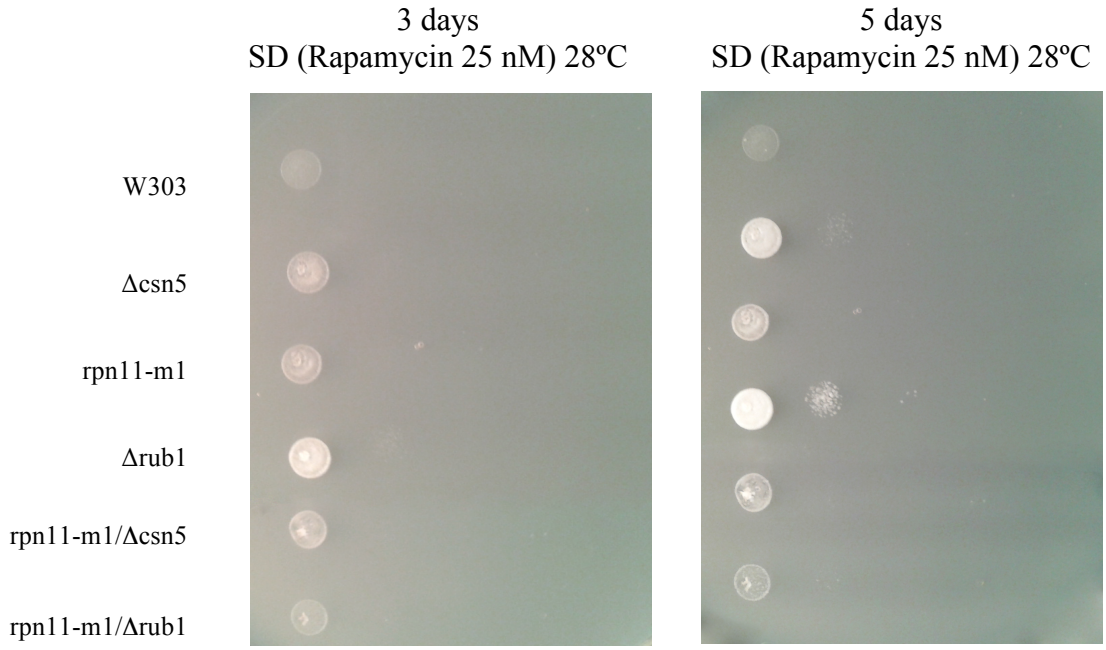

Figure 30. Serial dilutions, 10^7 cells/mL to 10^3 cells/mL spotted in SD (Rapamycin 25nM) medium plates, at 28ºC, after 3 and 5 days of growth. W303, rpn11-m1, Δrub1, rpn11-m1/Δcsn5 and rpn11-m1/Δrub1 strains are first inoculated in a concentration of 10^4 cells/mL. The cells were grown overnight in YPD medium at 28ºC in agitation and a 5 µl spot of each dilution is placed from the less diluted to the more dilute.

By observation of the Figure 30, after 5 days of grow, we see that Δcsn5 and Δrub1 show resistance to rapamycin comparing with the WT. This drug induces autophagy and,

in the case of Δcsn5, this resistance can be due to the fact that the cells are already in autophagy . However, as with MMS, we cannot take final conclusions, regarding the results due to the vast possibilities of action of these two drugs.

4.2.8 Mitophagy

A specific type of autophagy, mitophagy, targets mitochondria to be degraded in the cell. This process is an important subcellular event to maintain proper cellular homeostasis since this organelle is the major source of cellular reactive oxygen species (ROS). Mitophagy roles are essentially mitochondria quality control, elimination of mitochondria during development and when the organelle is in excess in the cell. Accumulation of damaged mitochondria is related with aging, certain types of cancer, neurodegenerative diseases and can also trigger apoptosis. Knowing that Δcsn5 enters in autophagy at an early stage and accounting for the growth defect in YPGly of Δrub1 and the double rpn11-m1/Δrub1 and rpn11-m1/Δcsn5 together with mitochondria morphology defects, we analyzed mitophagy in order to have a more precise ideia about mitochondria viability.

The autophagy-related gene 32 (Atg-32) is a mitochondrion outer membrane protein that is known to be active only in mitophagy induction through interaction with other proteins, such as Atg11. Therefore, Atg32 confers selectivity for mitochondria sequestration and degradation by the autophagy machinery and is identification provided some insight into the process of selecting and delivering mitochondrion to the vacuole in yeast [86,87]. Induction of mitophagy can be done by nitrogen starvation or use of rapamycin .

In order to investigate if our mutants undergo mitophagy we transformed with GFP-Atg32 and proceed with fluorescence microscopy and western blot analysis. For the microscopy assay, the cells were observed in exponential phase after grew at 28°C in YPD liquid medium plus adenine and stained with FM4-64 to allow the observation of the vacuole (Figure 31). The percentage of cells in mitophagy was also assessed and the results are shown in the Figure 32.

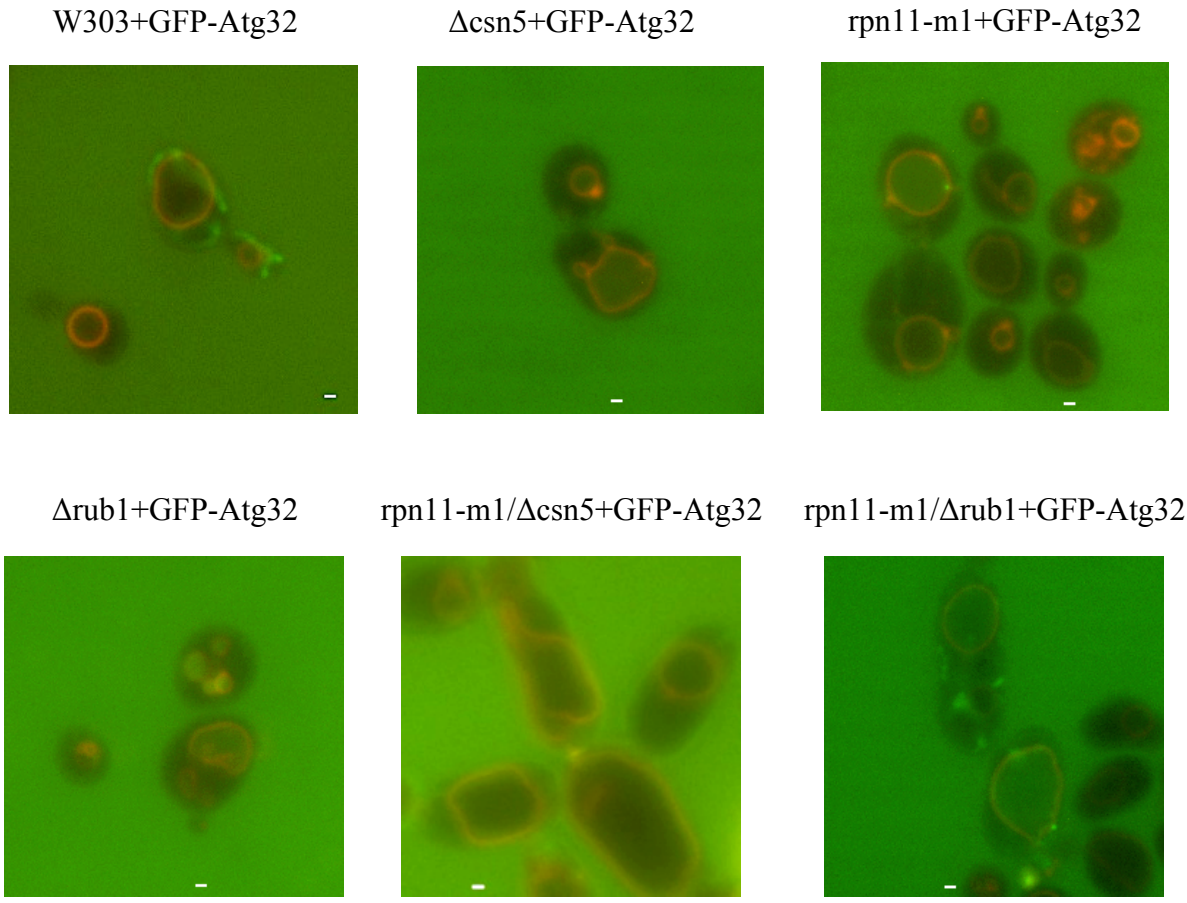

Figure 31. W303, rpn11-m1, Δrub1, rpn11-m1/Δcsn5 and rpn11-m1/Δrub1 strains transformed with GFP-Atg32 plasmid observed at the fluorescence microscope, in exponential phase, stained with FM4-64 dye for vacuole observation. The cells were grown overnight in YPD medium at 28ºC in agitation.

From the observation of the Figure 31 we see that the WT does not undergo mitophagy since de GFP is localized out of the vacuole. In the case of the singles and the double mutant rpn11-m1/Δrub1 we observed mitophagy since the GFP protein is present inside of the vacuole. To have a better understanding about the extension of this process in the cells we calculate a percentage of cells in mitophagy and the result is shown in the Figure 32 where we see that, as expected the WT has a very low percentage of cells in mitophagy, around 1.5 %, meanwhile the single mutants present mitophagy approximately 55%, 60% and 46% for Δcsn5, rpn11-m1 and Δrub1, respectively, a percentage that drops to 10% and 40% in the double mutants, rpn11-m1/Δcns5 and rpn11-m1/Δrub1, respectively.

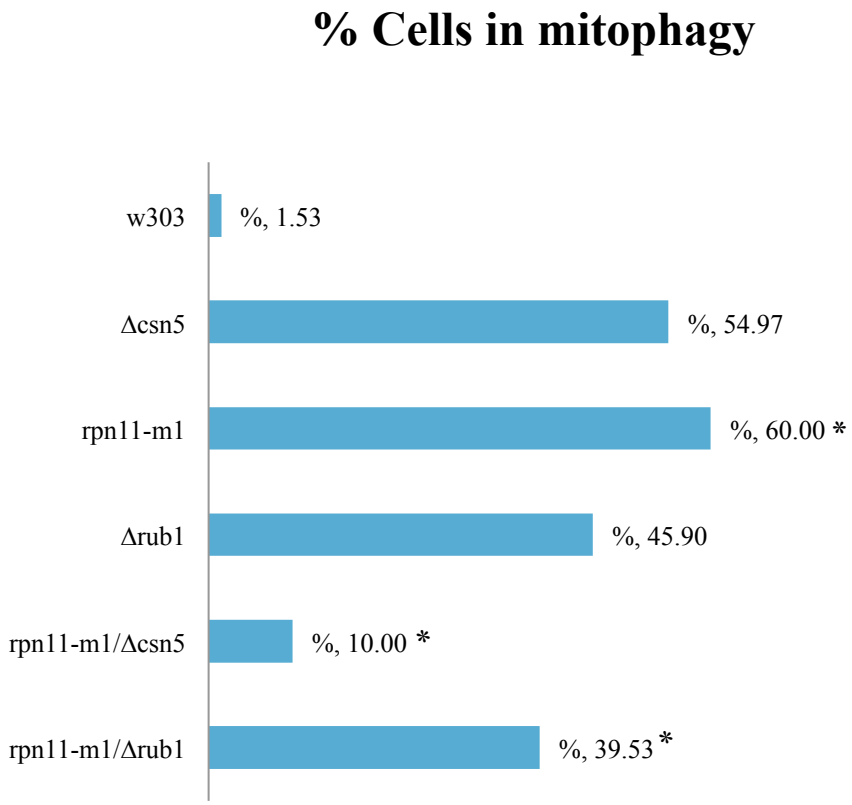

Figure 32. Wild-type (W303), single mutants (Δcsn5, rpn11-m1, Δrub1) and double mutants (rpn11-m1/Δcsn5, rpn11-m1/Δrub1) graphic of the cells in mitophagy (%). Cells were grown at 28ºC in YPD solid medium, in agitation.

Regarding the observation of autophagy in the Δcsn5 mutant, who indicates cellular stress, and previous studies on this mutant in the laboratory, we expected the observation of mitophagy, which was indeed confirmed. In the mutants indicated with an asterisk (*), the percentage was calculated in a base of less than 100 cells (See Appendix 2.2) due to the fact that, in the case of the double mutants, like we previously saw in the vitality test, we have growth defects which means a decrease in the number of living cells. In the case of rpn11-m1 we know that it has mitochondrial problems, not growing in glycerol base medium at non-permissive temperature, so is reasonable to think that it can present mitophagy. In the other hand, the Δrub1 mutant was not expectable to undergo mitophagy because it does not show respiration problems or decrease in the membrane potential or abnormal morphology when compare with the WT in the microscope observation with DASPMI coloration.

To confirm the observation of mitophagy we performed a western blot analysis using a primary antibody against the GFP, in cells grew in –URA selective medium (plasmid selection) at 28ºC, overnight in agitation, in exponential phase (1 day of growth), with the Ada2 gene as a control. The mutant Δcsn5, Δrub1 and rpn11-m1/Δcsn5 show a band for GFP-Atg32 and a band for GFP alone. The WT negative control, as expected, as no bands, a situation also present in the case of the double mutant rpn11-m1/Δrub1, that could be due to the low cell viability which leads to an inability to extract a significant amount of protein (See Appendix 1). In the case of the rpn11-m1 we see, like in the W303+GFP-Atg32, a unique band corresponding to GFP. From this western blot analysis we can say that Δcsn5 and Δrub1 clearly show mitophagy in exponential growth phase, confirming the fluorescence microscope analysis. These results are in concordance with the results obtained by Abeliovich, in a study that is still in development, giving us bases to confirm the influence of these two mutants in the mitochondrion function.

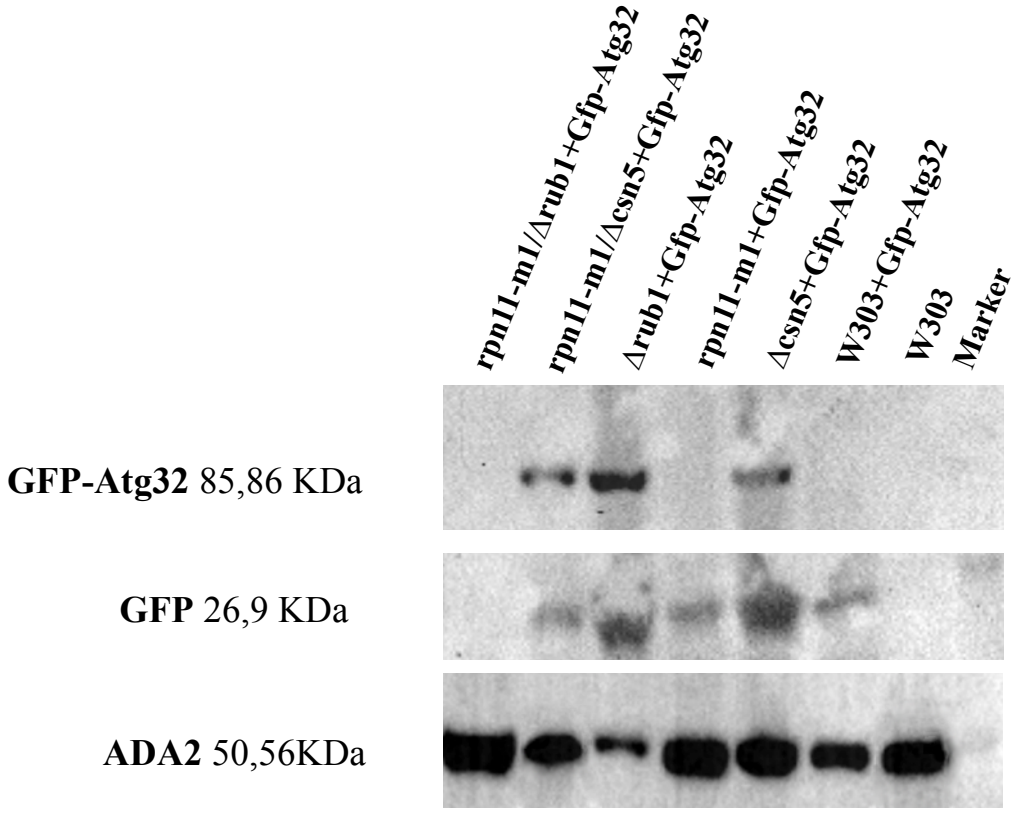

Figure 33.Western blot analysis on the strains W303, rpn11-m1, Δrub1, rpn11-m1/Δcsn5 and rpn11-m1/Δrub1 transformed with GFP-Atg32 plasmid after 1 day of growth in –URA selective medium, at 28ºC in agitation.

4.2.9 Reactive oxygen species (ROS)

Mitochondria convert energy for the cell into a usable form, ATP. The process of ATP formation is called oxidative phosphorylation (OXPHOS) and involves the transport of protons across the inner membrane by means of the electron transport chain. The final proton acceptor is an oxygen molecule that, in normal conditions is reduced to produce water. However, in some cases, the oxygen can be prematurely and incompletely reduced, forming superoxide radicals ($\bullet O_2^-$). Under normal physiological conditions, the cell has the capacity to balance the concentration of ROS but, under oxidative stress, excessive accumulation of ROS can damage cellular proteins, lipids and DNA, leading to aging, carcinogenesis and apoptosis [88,89] .

As we know, the mitochondrion is the major site of ROS production (mtROS), in which the superoxide radicals are quickly dismutated to hydrogen peroxide (H_2O_2) by two dismutases including superoxide dismutase 2 (SOD2) in the mitochondrial matrix and superoxide dismutase 1 (SOD1) in the mitochondrial intermembrane space [89] .

To investigate if, in our mutants, the production of ROS is causing an oxidative stress in the cell contributing to a decrease in viability we constructed two conditions: non-treated and treated cells with H_2O_2 followed by dihydrorhodamine coloration. In the presence of ROS this molecule is oxidated to rhodamine (See Appendix 3).

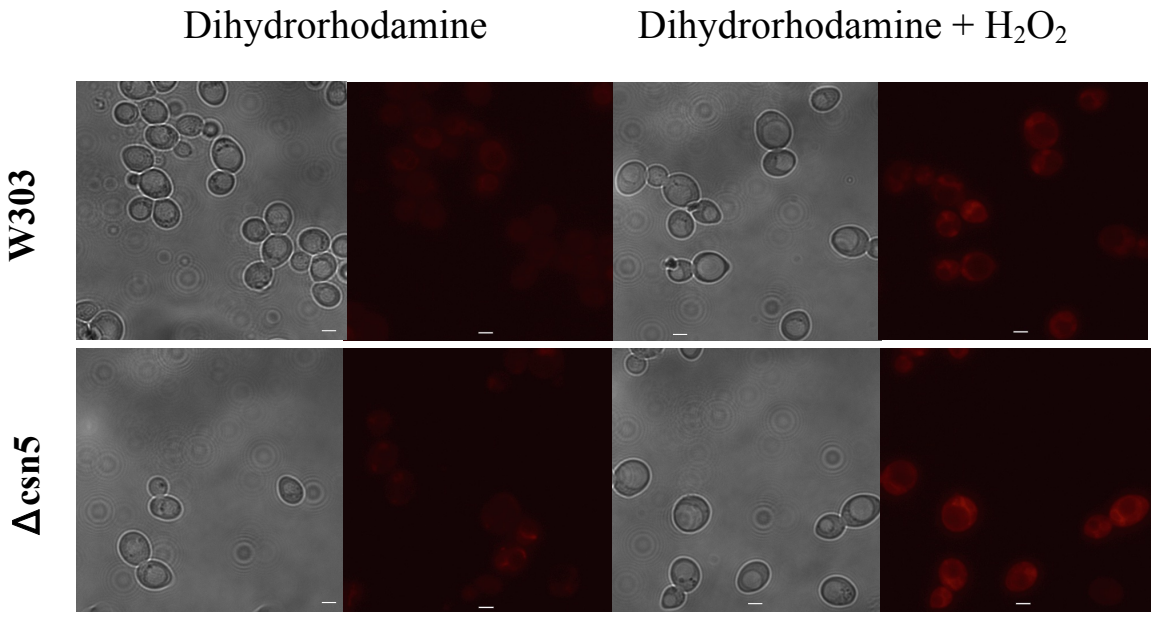

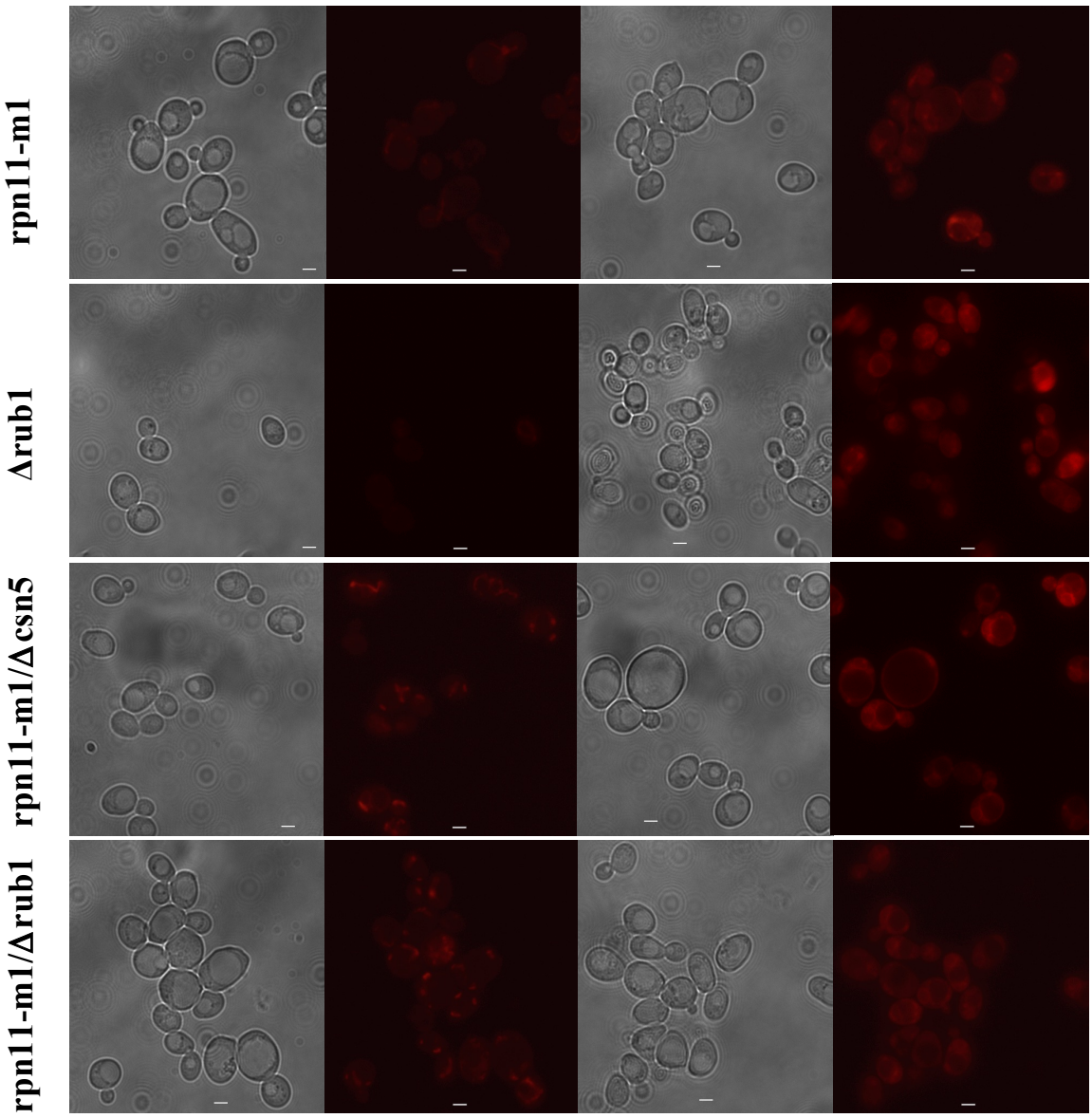

Figure 34. W303, rpn11-m1, Δrub1, rpn11-m1/Δcsn5 and rpn11-m1/Δrub1 strains at the conditions: dihydrorhodamine and dihydrorhodamine+H_2O_2. The cells were grown overnight in YPD medium at 28ºC in agitation and the scale bar is 0,2 μm for all the pictures (visible and fluorescence).

The obtained results revealed in the Figure 34, show that, in the double mutants there is a significant accumulation of ROS in the mitochondria in the non-treated cells, comparing with the cells treated with hydrogen peroxide that exhibit the presence of ROS throughout the cell. This scenario is not seen in the single mutants, Δcsn5 does not accumulate ROS in exponential phase, which tell us that the production of these molecules is not directly related with mitophagy as it is frequently thought. However, we can assume that the problems in the disposal of ROS in the mitochondrion in the case of the double mutants is somehow related with a decrease in cell viability and that this could be derived from the cumulative deficiency in the protein degradation due to the incapacity of CRL's recycling and the mutation in the deubiquitinase protein in the proteasome (Rpn11) that in the end cause the triggering of mitophagy in early stages.

5. Conclusions and Future Perspectives

In the course of this research I started by the characterization of the Δcsn5 mutant in *Saccharomyces cerevisiae*, in terms of phenotype, growth and capability to use different carbon sources and to maintain cellular homeostasis (autophagy). This study was made in comparison with the wild type strain (W303-1A) that shows a high capability of growth on both glucose and glycerol base medium and extended respiration, suggesting no defects on metabolic mitochondrial related functions. Has we know, the Csn5 subunit of the CSN complex, interacts in the ubiquitin-proteasome pathway by deneddylation of the Cdc53/Cul1 E3 ligase therefore promoting cycle completion that allows protein ubiquitination and subsequent degradation by the proteasome. In order to determine if the activity of this enzyme is somehow related with the Rpn11 subunit of the proteasome lid that performs deubiquitination and if the proteasome degradation is somehow linked with autophagy, more specifically, mitophagy, I studied a collection of mutants: rpn11-m1, Δrub1, rpn11-m1/Δcsn5 and rpn11-m1/Δrub1 together with Δcsn5 and the WT strain. Characterization of these strains was based in phenotype analysis, growth profile in optimal conditions (glucose rich medium at 28ºC) and in different carbon sources at permissive (28ºC) and non-permissive temperature (36º), DNA stability, genotoxic and proteoxic stress response and mitochondria potential defects together with cell viability (mitophagy and ROS).

The results demonstrate that the mutant rpn11-m1/Δrub1 is semi-lethal with growth difficulties in normal conditions, when compared with the other strains, and with an extreme phenotype showing aberrant cell morphology, low vitality and mitochondrial deficiency since it has problems on growing in glycerol rich medium at 28ºC. Also the double mutant rpn11-m1/Δcsn5 is problematic being sensitive to canavanine together with the single mutant Δcsn5. Interestingly, Δcsn5 is at the same time resistant to the DNA damaging agent MMS, suggesting a role on the control of the degradation of proteins involved in DNA repair. The demonstration, through western blot analysis that the double mutant rpn11-m1/Δcsn5 is engaged in early mitophagy indicates a cumulative defect in the control of cellular proteostasis, defect that is also seen in Δcsn5 and Δrub1. This fact leads to think about the importance in the balance between the rubylation/derubylation cycles and its role in the maintenance of cell vitality. Regarding the rpn11-m1/Δrub1, due to his growth problems we were not able to conclude if the mitophagy is physiological or if it is due to his semi-lethal phenotype.

In addition, this semi-lethal phenotype of the double mutants, frequent leads to the development of revertants, which is a drawback in their study requiring a constant screening.

It was also interesting to conclude that, not always, the production of ROS directly cause mitochondria imbalances, since we saw that in Δcsn5 and Δrub1 there are no ROS production but yet we have mitophagy.

In terms of futures perspectives I think it is important to do a more intensive study to understand the level of rubylated (Cdc53-Rub1) and non rubylated (Cdc53) E3 ligase in the double mutant rpn11-m1/Δcsn5, comparing with the single mutants rpn11-m1 and /Δcsn5. It would be also interesting to investigate effective Cdc53 substrates by affinity tests, tagging the protein Skp1, since there are much more F-box's which difficult the analysis, and make a pull-down in a chromatography column and then analyze the extract through mass spectrometry. This study could bring some highlights in the subject of the Δcsn5 resistance to MMS. In the other hand it is also important to continue with the work that is being developed in the overexpression of the CSN5 gene since it is a condition present in some human cancers. It could be also interesting to access the strains growth in glycose rich medium, also together with the analysis of rubylated and non rubylated E3 ligase.

Is important to notice that the ubiquitin-proteasome pathway is a complex network that involves a lot of factors and therefore is not easy to rapidly extract final conclusions and is because of this that the cellular biology study of specific proteasome and CSN mutants is crucial to began to understand their role in this conserved and essential cell process.

6. Bibliography

1. Amm, I., *et al*., Protein quality control and elimination of protein waste: the role of the ubiquitin-proteasome system. Biochim Biophys Acta, 2014. 1843(1): p. 182-96.
2. Wang, X., *et al*., Ubiquitin receptors and protein quality control. J Mol Cell Cardiol, 2013. 55: p. 73-84.
3. Yorimitsu, T., *et al*., Autophagy: molecular machinery for self-eating. Cell Death Differ, 2005. 12 Suppl 2: p. 1542-52.
4. Ciechanover, A., *et al*., The complexity of recognition of ubiquitinated substrates by the 26S proteasome. Biochim Biophys Acta, 2014. 1843(1): p. 86-96.
5. Nalepa, G., *et al*., Drug discovery in the ubiquitin-proteasome system. Nat Rev Drug Discov, 2006. 5(7): p. 596-613.
6. Merlet, J., *et al*., Regulation of cullin-RING E3 ubiquitin-ligases by neddylation and dimerization. Cell Mol Life Sci, 2009. 66(11-12): p. 1924-38.
7. Hilt, W., *et al*., Proteasomes: the world of regulatory proteolysis. Landes Bioscience, 2000.
8. Mandemakers, W., *et al*., A cell biological perspective on mitochondrial dysfunction in Parkinson disease and other neurodegenerative diseases. J Cell Sci, 2007. 120(Pt 10): p. 1707-16.
9. Glickman, M.H., *et al*., The ubiquitin-proteasome proteolytic pathway: destruction for the sake of construction. Physiol Rev, 2002. 82(2): p. 373-428.
10. Naujokat, C., *et al*., Role and function of the 26S proteasome in proliferation and apoptosis. Lab Invest, 2002. 82(8): p. 965-80.
11. Hochstrasser, M., There's the rub: a novel ubiquitin-like modification linked to cell cycle regulation. Genes Dev, 1998. 12(7): p. 901-7.
12. Lander, G.C., *et al*., Complete subunit architecture of the proteasome regulatory particle. Nature, 2012. 482(7384): p. 186-91
13. Bilotti, S.E.K.E., Novel Agents for the Treatment of Multiple Myeloma: Proteasome Inhibitors and Immunomodulatory Agents. Advanced Practitioner in Oncology, 2013. 4(5): p. 307-321.
14. Rinaldi, T., *et al*., Participation of the proteasomal lid subunit Rpn11 in mitochondrial morphology and function is mapped to a distinct C-terminal domain. Biochem J, 2004. 381(Pt 1): p. 275-85.
15. Berndt, C., *et al*., Ubiquitin system: JAMMing in the name of the lid. Curr Biol, 2002. 12(23): p. R815-7.

16. Rinaldi, T., *et al*., Dissection of the carboxyl-terminal domain of the proteasomal subunit Rpn11 in maintenance of mitochondrial structure and function. Mol Biol Cell, 2008. 19(3): p. 1022-31.

17. Esposito, M., *et al*., Analysis of the rpn11-m1 proteasomal mutant reveals connection between cell cycle and mitochondrial biogenesis. FEMS Yeast Res, 2011. 11(1): p. 60-71.

18. Rinaldi, T., *et al*., A mutation in a novel yeast proteasomal gene, RPN11/MPR1, produces a cell cycle arrest, overreplication of nuclear and mitochondrial DNA, and an altered mitochondrial morphology. Mol Biol Cell, 1998. 9(10): p. 2917-31.

19. Hofmann, L., *et al*., A nonproteolytic proteasome activity controls organelle fission in yeast. J Cell Sci, 2009. 122(Pt 20): p. 3673-83.

20. Spataro, V., K. Simmen, and C.A. Realini, The essential 26S proteasome subunit Rpn11 confers multidrug resistance to mammalian cells. Anticancer Res, 2002. 22(6c): p. 3905-9.

21. Budhidarmo, R., *et al*., RINGs hold the key to ubiquitin transfer. Trends Biochem Sci, 2012. 37(2): p. 58-65.

22. Soucy, T.A., *et al*., The NEDD8 Conjugation Pathway and Its Relevance in Cancer Biology and Therapy. Genes Cancer, 2010. 1(7): p. 708-16.

23. Bosu, D.R., *et al*., Cullin-RING ubiquitin ligases: global regulation and activation cycles. Cell Div, 2008. 3: p. 7.

24. Duda, D.M., *et al*., Structural insights into NEDD8 activation of cullin-RING ligases: conformational control of conjugation. Cell, 2008. 134(6): p. 995-1006.

35. Lanker, S., *et al*., Rapid degradation of the G1 cyclin Cln2 induced by CDK-dependent phosphorylation. Science, 1996. 271(5255): p. 1597-601.

26. Ho, M.S., *et al*., The utility F-box for protein destruction. Cell Mol Life Sci, 2008. 65(13): p. 1977-2000.

27. Ohki, Y., *et al*., The mechanism of poly-NEDD8 chain formation in vitro. Biochem Biophys Res Commun, 2009. 381(3): p. 443-7.

28. Yamoah, K., *et al*., Autoinhibitory regulation of SCF-mediated ubiquitination by human cullin 1's C-terminal tail. Proc Natl Acad Sci U S A, 2008. 105(34): p. 12230-5.

29. Morimoto, M., *et al*., Modification of cullin-1 by ubiquitin-like protein Nedd8 enhances the activity of SCF(skp2) toward p27(kip1). Biochem Biophys Res Commun, 2000. 270(3): p. 1093-6.

30. Deshaies, R.J., Drug discovery: Fresh target for cancer therapy. Nature, 2009. 458(7239): p. 709-710.

31. Siergiejuk, E., *et al*., Cullin neddylation and substrate-adaptors counteract SCF inhibition by the CAND1-like protein Lag2 in Saccharomyces cerevisiae. Embo j, 2009. 28(24): p. 3845-56.

32. Liakopoulos, D., *et al*., A novel protein modification pathway related to the ubiquitin system. Embo j, 1998. 17(8): p. 2208-14.

33. Lammer, D., *et al*., Modification of yeast Cdc53p by the ubiquitin-related protein rub1p affects function of the SCFCdc4 complex. Genes Dev, 1998. 12(7): p. 914-26.

34. Finley, D., *et al*., The ubiquitin-proteasome system of Saccharomyces cerevisiae. Genetics, 2012. 192(2): p. 319-60.

35. Chamovitz, D.A., *et al*., The COP9 complex, a novel multisubunit nuclear regulator involved in light control of a plant developmental switch. Cell, 1996. 86(1): p. 115-21.

36. Kotiguda, G.G., *et al*., The organization of a CSN5-containing subcomplex of the COP9 signalosome. J Biol Chem, 2012. 287(50): p. 42031-41.

37. Wei, N. *et al*., COP9: a new genetic locus involved in light-regulated development and gene expression in arabidopsis. Plant Cell, 1992. 4(12): p. 1507-18.

38. Freilich, S., *et al*., The COP9 signalosome is essential for development of Drosophila melanogaster. Curr Biol, 1999. 9(20): p. 1187-90.

39. Seeger, M., *et al*., A novel protein complex involved in signal transduction possessing similarities to 26S proteasome subunits. Faseb j, 1998. 12(6): p. 469-78.

40. Wei, N. and X.W. Deng, The COP9 signalosome. Annu Rev Cell Dev Biol, 2003. 19: p. 261-86.

41. Maytal-Kivity, V., *et al*., COP9 signalosome components play a role in the mating pheromone response of S. cerevisiae. EMBO Rep, 2002. 3(12): p. 1215-21.

42. Kato, J.Y., *et al*., Mammalian COP9 signalosome. Genes Cells, 2009. 14(11): p. 1209-25.

43. Richardson, K.S., *et al*., The emerging role of the COP9 signalosome in cancer. Mol Cancer Res, 2005. 3(12): p. 645-53.

44. Licursi, V., *et al*., The COP9 signalosome is involved in the regulation of lipid metabolism and of transition metals uptake in Saccharomyces cerevisiae. Febs j, 2014. 281(1): p. 175-90.

45. Pick, E., *et al*., PCI complexes: Beyond the proteasome, CSN, and eIF3 Troika. Mol Cell, 2009. 35(3): p. 260-4.

46. Wei, N., *et al*., The COP9 signalosome: more than a protease. Trends Biochem Sci, 2008. 33(12): p. 592-600.

47. Serino, G. *et al*., Duplication and familial promiscuity within the proteasome lid and COP9 signalosome kin complexes. Plant Sci, 2013. 203-204: p. 89-97.

48. Echalier, A., *et al*., Insights into the regulation of the human COP9 signalosome catalytic subunit, CSN5/Jab1. Proc Natl Acad Sci U S A, 2013. 110(4): p. 1273-8.

49. Tomoda, K., *et al*., The cytoplasmic shuttling and subsequent degradation of p27Kip1 mediated by Jab1/CSN5 and the COP9 signalosome complex. J Biol Chem, 2002. 277(3): p. 2302-10.

50. Tomoda, K., *et al*., Degradation of the cyclin-dependent-kinase inhibitor p27Kip1 is instigated by Jab1. Nature, 1999. 398(6723): p. 160-5.

51. Lee, M.H., *et al*., Roles of COP9 signalosome in cancer. Cell Cycle, 2011. 10(18): p. 3057-66.

52. Oh, W., *et al*., Jab1 induces the cytoplasmic localization and degradation of p53 in coordination with Hdm2. J Biol Chem, 2006. 281(25): p. 17457-65.

53. Tomoda, K., *et al*., Multiple functions of Jab1 are required for early embryonic development and growth potential in mice. J Biol Chem, 2004. 279(41): p. 43013-8.

54. Schneiter, R., Genetics, Molecular and Cell Biology of Yeast. 2004: Université de Fribourg Suisse. 86.

55. Goffeau, A., *et al*., Life with 6000 genes. Science, 1996. 274(5287): p. 546, 563-7.

56. Zemla, A., *et al*., CSN- and CAND1-dependent remodelling of the budding yeast SCF complex. Nat Commun, 2013. 4: p. 1641.

57. Gavin, A.C., *et al*., Functional organization of the yeast proteome by systematic analysis of protein complexes. Nature, 2002. 415(6868): p. 141-7.

58. Wee, S., *et al*., Conservation of the COP9/signalosome in budding yeast. BMC Genet, 2002. 3: p. 15.

59. Yu, Z., *et al*., Dual function of Rpn5 in two PCI complexes, the 26S proteasome and COP9 signalosome. Mol Biol Cell, 2011. 22(7): p. 911-20.

60. McBride, H.M., *et al*., Mitochondria: more than just a powerhouse. Curr Biol, 2006. 16(14): p. R551-60.

61. Westermann, B., Mitochondrial inheritance in yeast. Biochim Biophys Acta, 2013.

62. Taylor, E.B., *et al*., Mitochondrial quality control by the ubiquitin-proteasome system. Biochem Soc Trans, 2011. 39(5): p. 1509-13.

63. Benard, G., *et al*., Mitochondrial bioenergetics and structural network organization. J Cell Sci, 2007. 120(Pt 5): p. 838-48.

64. Boldogh, I.R., *et al*., Mitochondrial inheritance in budding yeast. Traffic, 2001. 2(6): p. 368-74.

65. Rinaldi, T., *et al*., Mitochondrial diseases and the role of the yeast models. FEMS Yeast Res, 2010. 10(8): p. 1006-22.

66. Kanki, T., *et al*., Atg32 is a mitochondrial protein that confers selectivity during mitophagy. Dev Cell, 2009, 17(1): 98-109.

67. Abeliovich, H., *et al.,* Chemical genetic analysis of Apg1 reveals a non-kinase role in the induction of autophagy. Mol Biol Cell, 2003, 14(2): 477-490.

68. Westermann, B., *et al*., Mitochondria-targeted green fluorescent proteins: convenient tools for the study of organelle biogenesis in Saccharomyces cerevisiae. Yeast, 2000, 16(15): 1421-1427.

69. Cebollero, E., *et al*., Regulation of autophagy in yeast Saccharomyces cerevisiae. Biochim Biophys Acta, 2009. 1793(9): p. 1413-21.

70. Shpilka, T., *et al*., Atg8: an autophagy-related ubiquitin-like protein family. Genome Biol, 2011. 12(7): p. 226.

71. Nair, U., *et al*., GFP-Atg8 protease protection as a tool to monitor autophagosome biogenesis. Autophagy, 2011. 7(12): p. 1546-50.

72. Klionsky, D.J., *et al*., Dynamic regulation of macroautophagy by distinctive ubiquitin-like proteins. Nat Struct Mol Biol, 2014. 21(4): p. 336-45.

73. Ulrich, H.D., Two-way communications between ubiquitin-like modifiers and DNA. Nat Struct Mol Biol, 2014. 21(4): p. 317-24.

74. Hammond-Martel, I., *et al*., Roles of ubiquitin signaling in transcription regulation. Cell Signal, 2012. 24(2): p. 410-21.

75. Ramadass, R., *et al*., How DASPMI reveals mitochondrial membrane potential: fluorescence decay kinetics and steady-state anisotropy in living cells. Biophys J, 2008. 95(8): p. 4068-76.

76. Solaini, G., *et al*., Evaluating mitochondrial membrane potential in cells. Biosci Rep, 2007. 27(1-3): p. 11-21.

77. Griffiths, E.J., Mitochondria - potential role in cell life and death. Cardiovascular Research, 2000. 46(1): p. 24-27.

78. Lundin, C., *et al*., Methyl methanesulfonate (MMS) produces heat-labile DNA damage but no detectable in vivo DNA double-strand breaks. Nucleic Acids Res, 2005. 33(12): p. 3799-811.

79. Wang, X., *et al*., Proteasomal degradation of Rpn4 in Saccharomyces cerevisiae is critical for cell viability under stressed conditions. Genetics, 2010. 184(2): p. 335-42.

80. Kolodner, R.D., *et al*., Maintenance of genome stability in Saccharomyces cerevisiae. Science, 2002. 297(5581): p. 552-7.

81. Michel, J.J., *et al*., A role for Saccharomyces cerevisiae Cul8 ubiquitin ligase in proper anaphase progression. J Biol Chem, 2003. 278(25): p. 22828-37.

82. Ben-Aroya, S., *et al*., Proteasome nuclear activity affects chromosome stability by controlling the turnover of Mms22, a protein important for DNA repair. PLoS Genet, 2010, 6(2): e1000852.

83. Karpov, D.S., *et al*., Proteasome inhibition enhances resistance to DNA damage via upregulation of Rpn4-dependent DNA repair genes. FEBS Lett, 2013. 587(18): p. 3108-14.

84. Kurmasheva, R. T., *et al*., Predicted mechanisms of resistance to mTOR inhibitors. Br J Cancer, 2006, 95(8): 955-960.

85. Nicklin, P., *et al*., Bidirectional transport of amino acids regulates mTOR and autophagy. Cel, 2009, 136(3): 521-534.

86. Kanki, T., *et al*., Atg32 is a tag for mitochondria degradation in yeast. Autophagy, 2009, 5(8): 1201-1202.

87. Kanki, T., *et al*., Mitochondria autophagy in yeast. Antioxid Redox Signal, 2011, 14(10): 1989-2001.

88. Mikkelsen, R. B., *et al*., Biological chemistry of reactive oxygen and nitrogen and radiation-induced signal transduction mechanisms. Oncogene 22(37): 5734-5754.

89. Li, X., *et al*., Targeting mitochondrial reactive oxygen species as novel therapy for inflammatory diseases and cancers. J Hematol Oncol, 2013, 6: 19.

7. Appendix

Appendix 1 (Bradford's Method)

mg/ml	0,25	0,5	1	2,5	5	10
BSA **(OD_{595})**	0,0199	0,0602	0,149	0,366	0,687	1,4803

	OD	mg/ml
W303	1,6714	8,57
W303+GFP-Atg32	1,1313	5,53
Δcsn5+GFP-Atg32	0,9196	4,34
rpn11-m1+GFP-Atg32	0,1975	0,29
Δrub+GFP-Atg32	1,4013	7,05
rpn11-m1/Δcsn5+GFP-Atg32	0,1864	0,23
rpn11-m1/Δrub+GFP-Atg32	0,1538	0,04

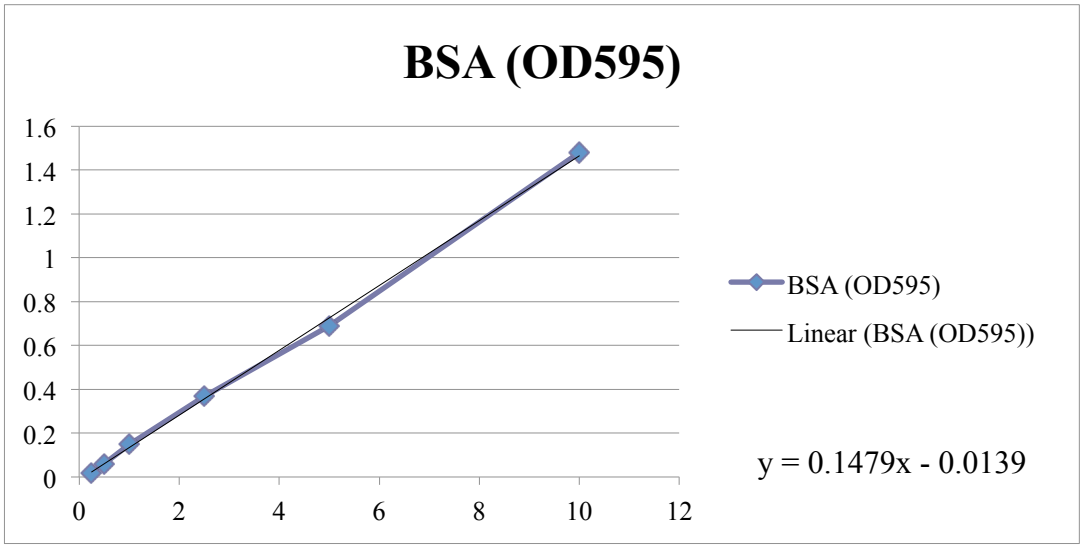

	x50ug (ml)
W303	0,0058
W303+GFP-Atg32	0,0090
Δcsn5+GFP-Atg32	0,0115
rpn11-m1+GFP-Atg32	0,1726
Δrub+GFP-Atg32	0,0071
rpn11-m1/Δcsn5+GFP-Atg32	0,2199
rpn11-m1/Δrub+GFP-Atg32	1,1272

Appendix 2

2.1 Vitality percentage (YPD, 28°C) for WT, single and double mutants:

Strain	% Media vitality YPD	%dev.st YPD	% Media (Normalized)
W303	69%	4%	100%
Δcsn5	49%	1%	71%
rpn11-m1	36%	3%	52%
Δrub1	50%	5%	73%
rpn11-m1/Δcsn5	41%	1%	60%
rpn11-m1/Δrub1	19%	1%	27%

2.2 Percentage of cells in mitophagy (YPD+adenine, 28°C) for WT, single and double mutants transformed with GFP-Atg32:

Strain	Cells in mitophagy	Total cells	%
W303+GFP-Atg32	3	196	1,53
Δcsn5+GFP-Atg32	83	151	54,97
rpn11-m1+GFP-Atg32	21	35	60,00
Δrub1+GFP-Atg32	56	122	45,90
rpn11-m1/Δcsn5+GFP-Atg32	1	10	10,00
rpn11-m1/Δrub1+GFP-Atg32	17	43	39,53

Appendix 3 (Dihydrorhodamine oxidation)

3.1 Dihydrorhodamine oxidation reaction (conversion in rhodamine)

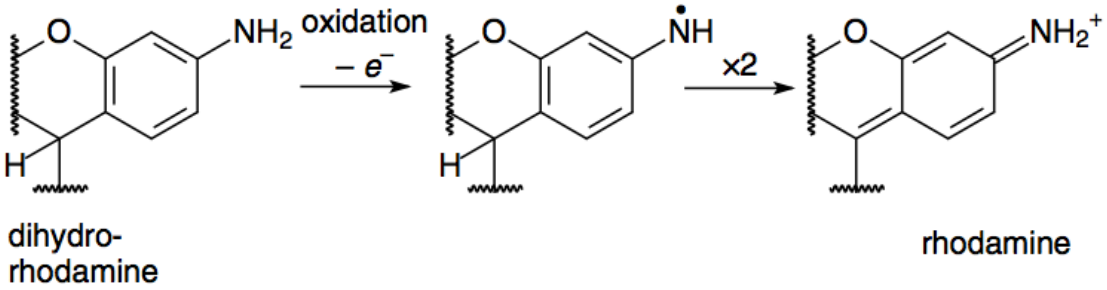

Bibliography (Appendix)

1. Mikkelsen, R. B. *et al*., (2003). "Biological chemistry of reactive oxygen and nitrogen and radiation-induced signal transduction mechanisms." Oncogene 22(37): 5734-5754.